

## Single channel properties of P2X ATP receptors in outside-out patches from rat hippocampal granule cells

Adrian Y. C. Wong, Geoffrey Burnstock\* and Alasdair J. Gibb

*Department of Pharmacology and \*Autonomic Neuroscience Institute, University College London, Gower Street, London WC1E 6BT, UK*

(Received 22 December 1999; accepted after revision 1 August 2000)

1. The single channel properties of P2X ATP receptors were investigated in outside-out patches from hippocampal granule cells in brain slices from 12-day-old rats. The results demonstrate that functional P2X ATP receptors are expressed in hippocampal granule cells and, combined with previously published information on the P2X subunits expressed in the hippocampus, suggest that the receptors may be heteromers of the P2X<sub>4</sub> and P2X<sub>6</sub> subunits or P2X<sub>1</sub>, P2X<sub>2</sub>, P2X<sub>4</sub> and P2X<sub>6</sub> subunits.
2. Two distinct types of P2X channel openings were observed. A flickery P2X receptor channel was observed in three patches with a mean chord conductance of  $32 \pm 6$  pS, a mean open time of  $1.0 \pm 0.3$  ms and a mean burst length of  $11 \pm 5$  ms at a membrane potential of  $-60$  mV. A large conductance P2X receptor was observed in 19 out of 98 patches with a mean conductance of  $56 \pm 1.8$  pS, a linear current–voltage relationship between  $-80$  and  $+60$  mV with a reversal potential around 0 mV, a mean open time of  $2.6 \pm 0.2$  ms and a mean burst length of  $8.8 \pm 1.8$  ms at  $-60$  mV. At an ATP concentration of 1 mM, these channels exhibited a low steady-state open probability ( $P_{\text{open}}$ ,  $0.07 \pm 0.008$ ;  $n = 15$ ), little apparent desensitisation and were also activated by  $\alpha,\beta$ -methylene ATP ( $\alpha,\beta$ -meATP,  $40 \mu\text{M}$ ;  $P_{\text{open}}$ ,  $0.007 \pm 0.0002$ ; conductance,  $57 \pm 1.1$  pS;  $n = 3$ ). No decrease in the single channel conductance was observed on increasing the free extracellular calcium concentration from 0.3 to 0.85 mM.
3. Channel closed time distributions were fitted with five exponential components with time constants (and relative areas) of 90  $\mu\text{s}$  (20%), 0.77 ms (32%), 10 ms (15%), 90 ms (18%) and 403 ms (15%) at 1 mM ATP. Of these, the first two components are suggested to represent gaps within single activations of the receptor based on the lack of agonist concentration dependence of these two shut time components between 1  $\mu\text{M}$  and 1 mM ATP.
4. Suramin (40  $\mu\text{M}$ ) significantly increased the single channel conductance ( $19 \pm 7\%$ ;  $n = 5$ ) and produced a small decrease in  $P_{\text{open}}$  ( $39 \pm 9\%$ ;  $n = 5$ ) by decreasing mean open time, burst length and total open time per burst. These actions of suramin are not consistent with simple competitive antagonism.

Binding sites for ATP that are thought to correlate with P2X receptors are widely distributed throughout the CNS (Bo & Burnstock, 1994; Balcar *et al.* 1995) and many CNS neurons express the mRNA (Collo *et al.* 1996) and protein for one or more of the P2X receptor subunits (Vulchanova *et al.* 1996; Lê *et al.* 1998b). Neurons in the adult rat hippocampus have been shown to express mRNA encoding the P2X<sub>4</sub> and P2X<sub>6</sub> receptor subunits (Collo *et al.* 1996), and additionally, mRNA encoding the P2X<sub>1</sub> and P2X<sub>2</sub> subunits has been observed in neonatal rat hippocampus (Kidd *et al.* 1995). Subunit-specific antibodies against the P2X<sub>4</sub> subunit have also confirmed the presence of this subunit in hippocampal neurons (Lê *et al.* 1998b). Electrophysiological studies of homomeric P2X receptors expressed in frog

oocytes and mammalian cell lines have provided insights into their functional characteristics and have shown that P2X<sub>1</sub> receptor subunit homomers differ from the homomeric P2X<sub>4</sub> and P2X<sub>6</sub> receptors in a number of ways. Firstly, recombinant homomeric P2X<sub>1</sub> receptors exhibit rapid desensitisation and are sensitive to the synthetic agonist  $\alpha,\beta$ -methylene ATP ( $\alpha,\beta$ -meATP; Valera *et al.* 1994) while the homomeric P2X<sub>4</sub> and P2X<sub>6</sub> receptors show very slow desensitisation and are not sensitive to  $\alpha,\beta$ -meATP (Bo *et al.* 1995; Collo *et al.* 1996). Secondly, homomeric P2X<sub>1</sub> receptors are sensitive to the antagonists suramin and PPADS (Valera *et al.* 1994), but recombinant P2X<sub>4</sub> and P2X<sub>6</sub> homomeric receptors are insensitive to these compounds (Bo *et al.* 1995; Collo *et al.* 1996), while heteromeric P2X<sub>4/6</sub>

receptors are weakly sensitive to suramin (Lê *et al.* 1998a). In contrast to homomeric P2X<sub>1</sub> receptors, P2X<sub>2</sub> receptors are insensitive to  $\alpha,\beta$ -meATP. Recent co-immunoprecipitation experiments using tagged P2X receptor protein have found that the P2X<sub>4</sub> receptor subunit only forms heteromultimers with the P2X<sub>5</sub> and P2X<sub>6</sub> receptor subunits, suggesting that there are specific interactions between subunits that control which subunits can form functional receptors (Torres *et al.* 1999). In addition, the work of Torres *et al.* (1999) suggests that P2X<sub>6</sub> subunits do not homo-oligomerise.

While there is ample evidence for the existence of functional P2X receptors in peripheral neurons (reviewed by Sneddon *et al.* 1996; Hoyle, 1996) and in brainstem nuclei, e.g. the locus coeruleus (Shen & North, 1993), there are only a few reports showing that functional P2X receptors exist in higher brain centres. P2X receptor-mediated calcium fluxes have been described in cultured cerebellar Purkinje cells (Mateo *et al.* 1998) and single channel currents mediated by P2X receptors from both Purkinje and cerebellar granule cells (Halliday & Gibb, 1997) have been observed. Synaptic transmission mediated by P2X receptors has been observed in the medial habenula (Edwards *et al.* 1992, 1997), spinal cord dorsal horn (Bardoni *et al.* 1997) and at some hippocampal Schaffer collateral-CA1 cell synapses (Pankratov *et al.* 1998).

Despite the evidence for expression of P2X receptor subunit mRNA and protein in the hippocampus, there is no information currently available concerning the single channel properties of P2X receptors in this brain region. The aim of the present study was to investigate the single channel properties of P2X receptors from dentate gyrus granule cells in hippocampal slices, and to compare the properties of these native receptors with those of P2X receptors expressed in recombinant systems. The results of these experiments provide detailed functional information on the properties of hippocampal P2X receptors and allow inferences to be made concerning the molecular composition of these receptors. Abstracts of some of these results have already been presented (Wong *et al.* 1998, 1999).

## METHODS

### Patch-clamp recording in brain slices

Patch-clamp recordings were made at room temperature (21–24 °C) using brain slices obtained from 12-day-old Sprague-Dawley rats as previously described (Edwards *et al.* 1989). Rats were decapitated and 250  $\mu$ m thick transverse slices of hippocampus were made in Krebs solution. Patch pipettes were pulled from borosilicate glass capillaries (Clark Electromedical GC150F-7.5) using a two-stage vertical puller (Narishige PP-83) coated with Sylgard (Dow Corning) and fire polished (Narishige MF-83) to a final tip diameter of around 1  $\mu$ m. Pipettes had resistances of 12–16 M $\Omega$  when filled with internal solution. Dentate gyrus granule cells were identified visually using a Zeiss Axioskop FS microscope equipped with Nomarski differential interference contrast optics with a total magnification of  $\times$ 640. Outside-out patches were formed from granule cells within the slice without prior cleaning following the

method described by Hamill *et al.* (1981). Patches with resistances of greater than 50 G $\Omega$  were used for these experiments.

### Solutions

The Krebs solution used for making brain slices had the following composition (mM): NaCl 125, NaHCO<sub>3</sub> 25, D-(+)-glucose 25, KCl 2.5, NaH<sub>2</sub>PO<sub>4</sub> 1.25, CaCl<sub>2</sub> 1 and MgCl<sub>2</sub> 2. The Krebs solution used during patch-clamp recording contained (mM): NaCl 125, NaHCO<sub>3</sub> 25, D-(+)-glucose 25, KCl 2.5, NaH<sub>2</sub>PO<sub>4</sub> 1.25 and CaCl<sub>2</sub> 1, and had a pH of 7.4 following gassing with 95% O<sub>2</sub>–5% CO<sub>2</sub>. All the reagents were from BDH (Poole, UK) and of AnalaR grade. The pipette solution consisted of (mM): CsCl 140, EGTA 10, Hepes 10 and CaCl<sub>2</sub> 1, adjusted to pH 7.3 using CsOH. ATP or  $\alpha,\beta$ -meATP was bath applied in the presence of 10  $\mu$ M 5,7-dichlorokynurenic acid (5,7-CK; Tocris) and 40  $\mu$ M bicuculline methiodide (Sigma) to outside-out patches by manually switching a tap in the inflow to the recording chamber. In order to prevent degradation of ATP due to spontaneous hydrolysis or the action of ectonucleotidases within the slice, an ATP regenerating solution was made (MacDonald *et al.* 1989a) by including 20 mM phosphocreatine and 10 units ml<sup>-1</sup> of creatine phosphokinase in addition to 1 mM ATP (all reagents from Sigma) in the recording Krebs solution. Suramin (40  $\mu$ M; Bayer) was bath applied for at least 1 min before any agonist introduction. The free calcium concentration in the extracellular solution was calculated using the program ALEX written by Michel Vivaudou (Commissariat à l'Énergie Atomique, Grenoble, France), which is based on the work of Fabiato (1988). Stability constants for HCO<sub>3</sub><sup>-</sup>, HPO<sub>4</sub><sup>-</sup>, ATP and phosphocreatine were taken from Smith & Martell (1982). The free extracellular Ca<sup>2+</sup> concentration was estimated to be 0.3 mM when the ATP concentration was 1 mM, and 0.85 mM when the ATP concentration was 40 and 1  $\mu$ M.

### Data acquisition and analysis

Single channel currents were amplified using an Axopatch 200A Integrating Patch Clamp (Axon Instruments), filtered at 10 kHz (–3 dB) by an 8th order low-pass Bessel filter and stored on digital audio tape using a digital tape recorder (Biologic DTR-1202). Selected recordings were replayed, filtered at 2 kHz (–3 dB, Bessel) and digitised at 20 kHz using a CED 1401+ digital interface (Cambridge Electronic Design) connected to a Dell XPS P133c computer, and stored on hard disk.

Following digitisation, single channel records were analysed by the time course-fitting method using the single channel analysis program SCAN (Colquhoun & Sigworth, 1995). Open time, shut time and burst length distributions are displayed logarithmically binned with a square root transformation of the ordinate (McManus *et al.* 1987; Sigworth & Sine, 1987). Channel openings are referred to as 'apparent openings' where appropriate to indicate that many observed openings are likely to contain unresolved gaps. Dwell time distributions were fitted using the program EKDIST with a mixture of exponential components using the maximum likelihood method (Colquhoun & Sigworth, 1995). Open–shut point amplitude distributions, and distributions of amplitudes measured by time course fitting were constructed using openings and closings longer than 2.0 filter rise times ( $t_r = 0.332$  ms) and fitted with two or three Gaussian components using the maximum likelihood method. Distributions of the number of openings in bursts of openings were fitted with two geometric components.

The open probability of the channel ( $P_{\text{open}}$ ) in the presence of ATP was calculated by dividing the mean open time by the sum of the mean open time and mean shut time. Mean open and shut times were calculated by integration of the exponential components fitted to open and shut time distributions, respectively.

Statistical analysis was by Student's paired two-tailed *t* test and a *P* value of  $\leq 0.05$  was considered significant. The slopes of the linear regression lines were tested for significance using an *F* test.

### Definition of bursts

Bursts of openings were defined as openings separated by closed times shorter than a critical length,  $t_{\text{crit}}$  (Colquhoun & Sakmann, 1985). This was calculated so as to make the percentage of long closed times that were misclassified as being within bursts equal to the percentage of short closed times that were misclassified as being between bursts (Colquhoun & Sakmann, 1985). For each patch containing large conductance P2X receptors, the  $t_{\text{crit}}$  was calculated from the best-fit parameters of the shut time distribution, treating the second and third fastest components as being 'within bursts' and 'between bursts' respectively. For patches containing the flickery P2X receptor,  $t_{\text{crit}}$  was calculated in an analogous way, using components three and four of the shut time distribution.

## RESULTS

Single channel recordings from native tissue preparations have demonstrated that ATP is able to activate channels with conductances between 9 and 63 pS (Benham & Tsein, 1987; Krishtal *et al.* 1988; Fieber & Adams, 1991; Silinsky & Gerzanich, 1993; Nakazawa & Hess, 1993) in 1 or 2 mM external  $\text{Ca}^{2+}$ . These conductances differ from those of recombinant homomeric P2X<sub>1</sub>, P2X<sub>2</sub>, P2X<sub>3</sub> or P2X<sub>4</sub> receptors expressed in CHO cells, which varied from 9 to 21 pS in 0.3 mM external  $\text{Ca}^{2+}$  (Evans, 1996), and P2X<sub>2</sub> receptors expressed in *Xenopus* oocytes where the conductance was 28 pS in zero external calcium (Zhou & Hume, 1998) or in HEK cells where the conductance was 20 pS in 1 mM external  $\text{Ca}^{2+}$  (Zhou & Hume, 1998). In patches from hippocampal granule cells, we also found that the conductance of native P2X receptors differed from that of homomeric recombinant receptors.

### Single channel conductance of large conductance P2X receptors

Figure 1 shows a representative recording from a hippocampal granule cell outside-out patch exposed to 1 mM ATP. Figure 1A illustrates the activation of channels observed on bath application of ATP. Figure 1B shows a continuous recording of 65 s of data at a membrane potential of  $-60$  mV. Channel openings were, on average, 3.1 pA in amplitude at this membrane potential. There were at least two channels present in the patch, as a small number of double openings were observed. This is interesting given the fact that 1 mM ATP evoked channel openings in only 15 out of 94 patches. In the absence of extracellular ATP, channel openings were rare (mean  $\pm$  s.e.m. of  $0.9 \pm 0.03$  s<sup>-1</sup>) and often were of different amplitude to channels activated by ATP, as illustrated in Fig. 1A during the 30 s of recording prior to ATP application. In the presence of 1 mM ATP, channel openings were mainly to one conductance level, although in 10 of the 15 patches obtained at this agonist concentration, a subconductance level was occasionally observed with an amplitude of 2.8 pA. For the 15 patches challenged with

1 mM ATP,  $P_{\text{open}}$  was  $0.07 \pm 0.008$ , with an opening frequency of  $15.7 \pm 2.29$  s<sup>-1</sup>. This is a statistically significant increase in activity compared to control recordings (paired *t* test;  $P < 0.05$ ). Thus, ATP application produced an approximately 20-fold increase in channel activity.  $P_{\text{open}}$  was agonist concentration dependent, as illustrated in Fig. 1C. For the four patches exposed to 1 or 40  $\mu\text{M}$  ATP,  $P_{\text{open}}$  was  $0.005 \pm 0.001$  (opening frequency,  $2.4 \pm 0.76$  s<sup>-1</sup>) and  $0.03 \pm 0.01$  (opening frequency,  $12.2 \pm 5.64$  s<sup>-1</sup>), respectively. The results suggest an  $\text{EC}_{50}$  of around 40  $\mu\text{M}$  for ATP at these receptors (assuming 1 mM ATP produces maximal steady-state channel activation). The ATP-induced increase in both  $P_{\text{open}}$  and opening frequency was statistically significant (unpaired *t* test;  $P < 0.05$ ).

Figure 1D shows the open–shut point amplitude distribution measured in this patch at a membrane potential of  $-60$  mV. For 15 patches in the presence of 1 mM ATP at  $-60$  mV the mean amplitude (and relative area) was  $3.36 \pm 0.11$  pA ( $95 \pm 1\%$ ). For 10 of these 15 patches a subconductance level of  $2.82 \pm 0.19$  pA ( $8 \pm 1\%$ ) was observed. Since the occurrence of the sublevel was relatively rare, channel shut time and channel burst analyses were performed without distinguishing between conductance levels. The proportion of sublevel openings increased as the ATP concentration was reduced and the mean amplitude of channel openings showed a slight concentration dependence, having an amplitude of  $3.4 \pm 0.11$  pA in the presence of 40  $\mu\text{M}$  ATP, and  $3.05 \pm 0.1$  pA in 1  $\mu\text{M}$  ATP.

The qualitative effect of changing the membrane potential on the channel properties of large conductance P2X receptors is shown in Fig. 2A. The traces suggest that there is an increase in the mean open time of the receptor at more depolarised voltages, and that the reversal potential of the channel is around 0 mV. It is also clear that the large conductance P2X receptor from hippocampal granule cells is also able to pass current at positive membrane potentials (Fig. 2B), unlike some native P2X receptors in other neuronal cell types (Krishtal *et al.* 1988; Bean *et al.* 1990; Silinsky & Gerzanich, 1993) or recombinant P2X<sub>2</sub> receptors where rectification of the single channel current is marked (Zhou & Hume, 1998; Ding & Sachs, 1999).

Figure 2B shows the single channel current–voltage relationship for P2X receptors in outside-out patches, where the external solution contained 0.3 mM free  $\text{Ca}^{2+}$  and 1 mM ATP. The data were fitted with a linear regression line producing a slope conductance of 55 pS with a reversal potential of  $+2.0$  mV. This corresponds well with the chord conductance of the channel, which was  $56 \pm 1.8$  pS measured at  $-60$  mV, assuming a reversal potential of 0 mV ( $n = 15$ ). The individual current–voltage relationships for five patches where recordings were made between  $-90$  and  $-30$  mV are illustrated in Fig. 2C and the slopes of the regression lines give a mean slope conductance of  $54 \pm 3.6$  pS. P2X receptor channels with a linear single

channel current–voltage relationship have been observed in smooth muscle (Benham & Tsein, 1987), cardiac ganglia (Fieber & Adams, 1991) and myenteric neurons (Zhou & Galligan, 1996). However, the single channel conductance observed in this study has not previously been observed in other native tissue preparations. In addition, increasing the extracellular  $\text{Ca}^{2+}$  concentration has been shown to

markedly reduce the conductance of P2X receptors in PC12 cells (Nakazawa & Hess, 1993) and sensory ganglia (Krishtal *et al.* 1988). However, this does not seem to be the case for hippocampal granule cell P2X receptors, as when the free  $\text{Ca}^{2+}$  concentration was increased from 0.3 mM to 0.85 mM, no significant decrease in single channel conductance was observed ( $56 \pm 1.8$  pS in 1 mM  $\text{Ca}^{2+}$ ;  $n = 4$ ;  $P > 0.05$ ).

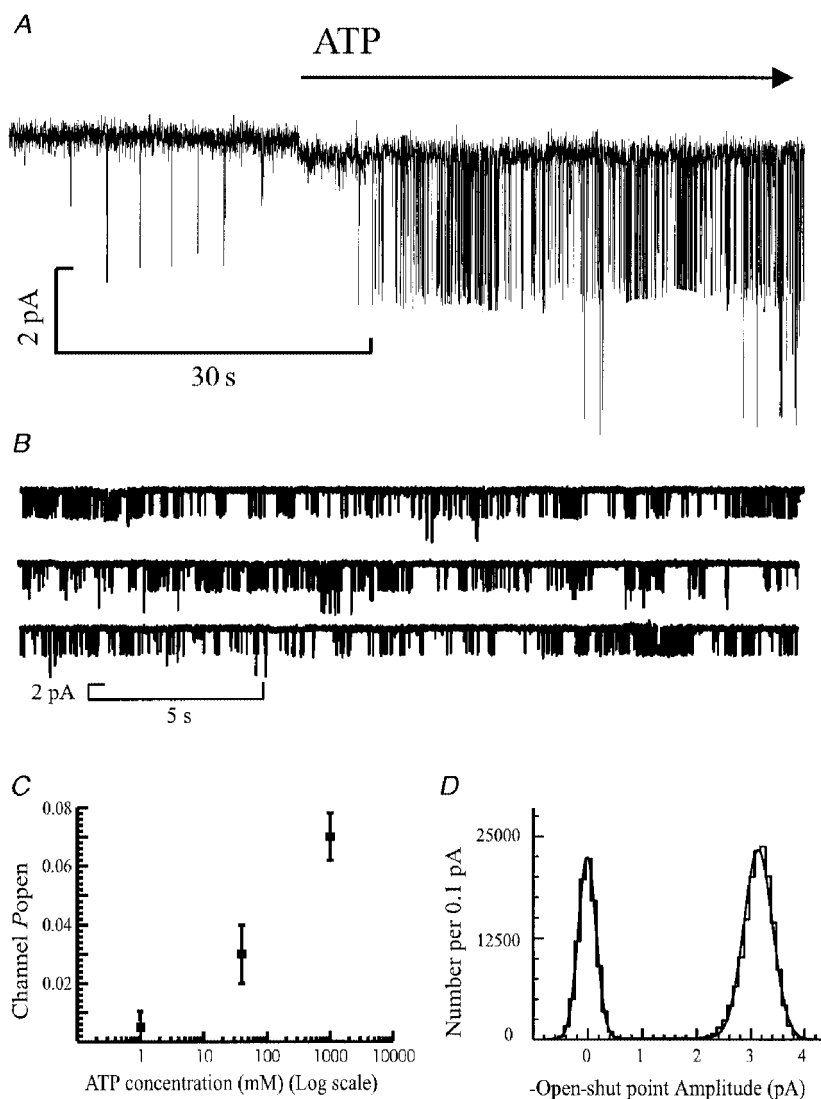


**Figure 1.** Activation by ATP of single channel currents in hippocampal granule cell outside-out patches

Single channel currents were activated by 1 mM ATP in the presence of  $10 \mu\text{M}$  5,7-CK and  $40 \mu\text{M}$  bicuculline. Membrane potential,  $-60$  mV. Free extracellular  $\text{Ca}^{2+}$  concentration, 0.3 mM. Channel openings appear as downward deflections from the baseline. *A*, channels are activated by ATP. The open probability ( $P_{\text{open}}$ ) before bath application of 1 mM ATP was 0.0007. ATP was added to the bath at the point indicated by the start of the arrow. *B*, successive horizontal traces showing three contiguous sweeps of 21 s duration to demonstrate typical channel activity seen at this concentration of ATP. In the presence of ATP,  $P_{\text{open}}$  was 0.095 with an opening frequency of  $19.5 \text{ s}^{-1}$ . Currents were low-pass filtered at 2 kHz ( $-3$  dB) and digitised at 20 kHz. *C*, the effect of increasing ATP concentration on  $P_{\text{open}}$  of the channel. The mean  $P_{\text{open}}$  was  $0.005 \pm 0.001$ ,  $0.03 \pm 0.01$  and  $0.06 \pm 0.008$  in the presence of  $1 \mu\text{M}$ ,  $40 \mu\text{M}$  and 1 mM ATP, respectively. Data points are means  $\pm$  s.e.m. from four patches at 1 and  $40 \mu\text{M}$  ATP, and 15 patches in the presence of 1 mM ATP. *D*, open–shut point amplitude distribution of 3725 channel openings of duration longer than two filter rise times ( $t_r = 0.332$  ms), measured from the same patch as illustrated in *A*. The distribution was fitted with the sum of two Gaussian components with fitted parameters of 0.01 pA (relative area, 36%; s.d. = 0.17 pA) and 3.1 pA (54%; s.d. = 0.27 pA).

### Kinetic analysis of large conductance channels

The distributions of apparent open times and closed times contain information relevant to the channel activation mechanism and in particular allow prediction of the number of shut states occupied by the receptor during activation and identification of the groups of openings (referred to as

'bursts') which occur during a single activation of the receptor (Colquhoun & Hawkes, 1981, 1982). In total we studied 15 patches exposed to 1 mM ATP. Four of these patches were also tested with 40  $\mu$ M ATP and, in addition, four other patches were tested only with 1  $\mu$ M ATP. Following analysis of the distributions of channel shut times

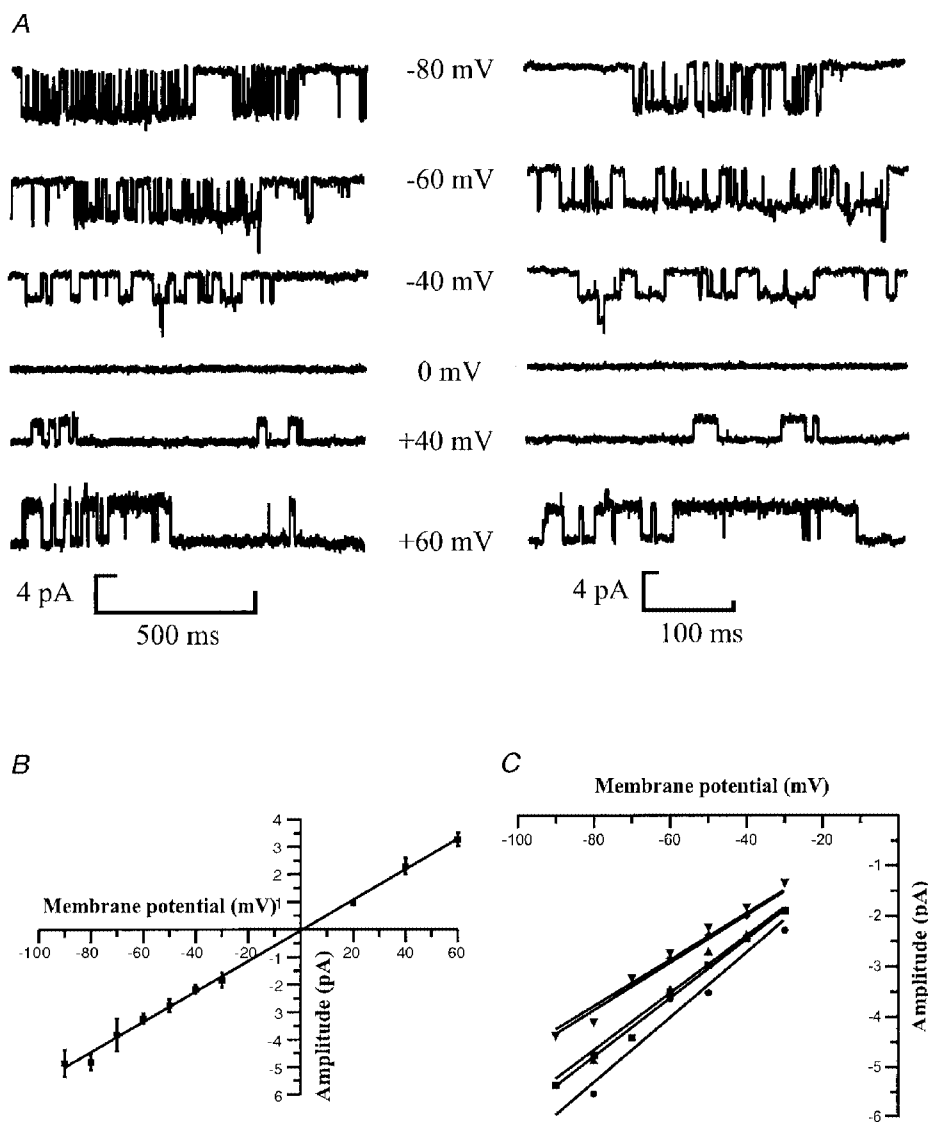


**Figure 2.** Dependence of channel amplitude on membrane potential

*A*, single channel currents were activated by 1 mM ATP in the presence of 10  $\mu$ M 5,7-CK, with a free  $\text{Ca}^{2+}$  concentration of 0.3 mM. Recordings are from an outside-out patch clamped at the membrane potentials shown beside the traces. Channel openings appear as downward deflections from the baseline at negative membrane potentials, and upward deflections from the baseline at positive membrane potentials. The left panel shows horizontal sweeps of 1100 ms to demonstrate channel activity at each membrane potential, and the right panel shows 400 ms traces of channel openings. Current records were low-pass filtered at 2 kHz ( $-3$  dB) and digitised at 20 kHz. *B*, relationship between single channel current amplitude and patch potential for five separate patches. Data points are means  $\pm$  s.e.m. of the mean single channel current obtained from Gaussian fits to the open–shut point amplitude distribution obtained at each membrane potential. The points were fitted with a linear regression line that predicts a slope conductance of 55 pS with a reversal potential of +2.0 mV. *C*, individual current–voltage relationships for each of five patches between  $-90$  and  $-30$  mV. The symbols represent mean single channel current obtained from Gaussian fits of the amplitude distribution at each patch potential. The points are fitted with linear regression lines constrained to cross the ordinate at +2.0 mV. The slopes of the regression lines give a mean slope conductance of  $54 \pm 3.6$  pS.

and open times, the distributions of burst lengths, total open time per burst and number of openings per burst were analysed.

**Shut time distributions.** Distributions of shut times, such as those shown in Fig. 3*A* and *B*, were best fitted with the sum of five exponential components at all three concentrations of ATP tested. At  $1\ \mu\text{M}$  ATP these had time constants (and relative areas) of  $\tau_1 = 63 \pm 14\ \mu\text{s}$  ( $20 \pm 3.5\%$ ),  $\tau_2 = 0.92 \pm 0.04\ \text{ms}$  ( $52 \pm 2.1\%$ ),  $\tau_3 = 18 \pm 4.2\ \text{ms}$  ( $5.9 \pm 0.9\%$ ),  $\tau_4 = 715 \pm 354\ \text{ms}$  ( $9.4 \pm 2.3\%$ ) and  $\tau_5 = 3433 \pm$

$1192\ \text{ms}$  ( $13 \pm 1.9\%$ ). The distribution means averaged  $515 \pm 185\ \text{ms}$ . At  $1\ \text{mM}$  ATP, the exponential components had time constants (and relative areas) of  $\tau_1 = 90 \pm 10\ \mu\text{s}$  ( $20 \pm 1.9\%$ ),  $\tau_2 = 0.76 \pm 0.09\ \text{ms}$  ( $32 \pm 4.3\%$ ),  $\tau_3 = 10 \pm 2.1\ \text{ms}$  ( $15 \pm 1.6\%$ ),  $\tau_4 = 90 \pm 24\ \text{ms}$  ( $18 \pm 2.6\%$ ) and  $\tau_5 = 403 \pm 103\ \text{ms}$  ( $15 \pm 2.4\%$ ). The distribution means averaged  $62 \pm 10\ \text{ms}$  (Table 1).

The time constants of the two shortest components were found not to vary significantly (Student's *t* test;  $P > 0.05$ ) with agonist concentration (Fig. 3*C*). The third exponential

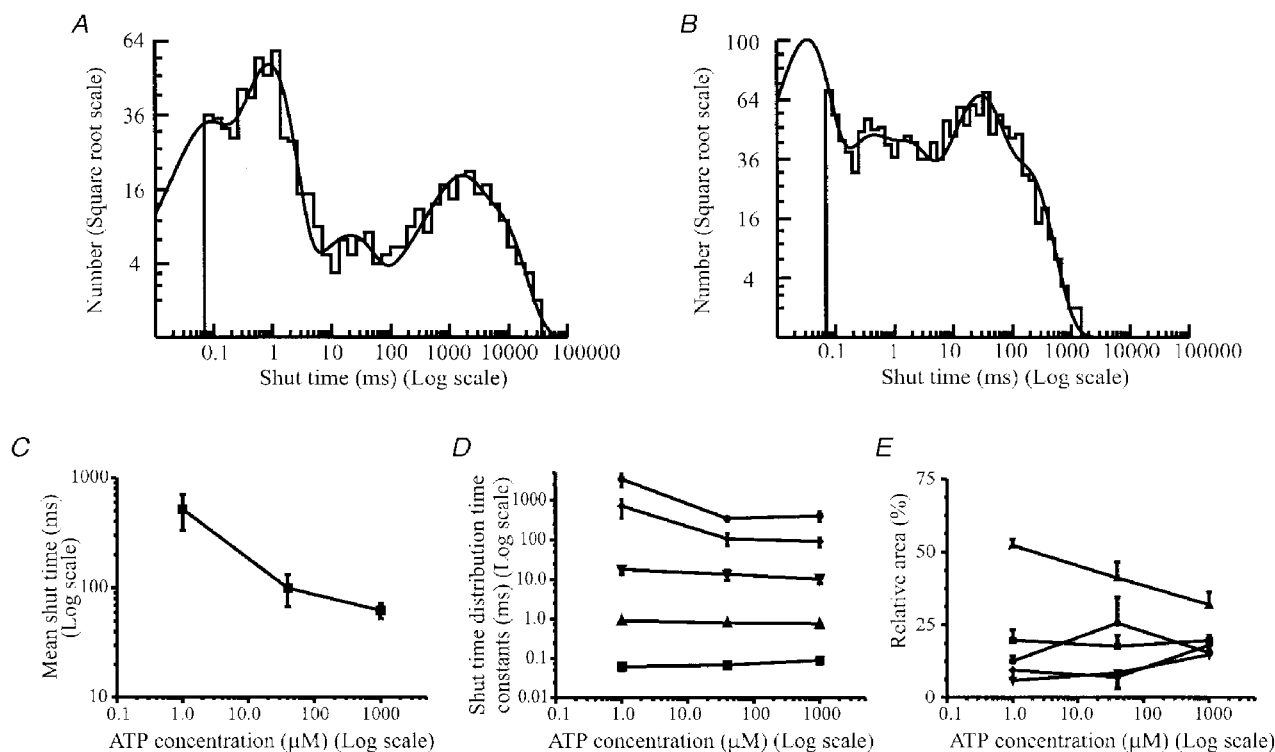


**Figure 3.** Agonist concentration dependence of P2X receptor shut times

*A*, distribution of all shut times greater than  $70\ \mu\text{s}$  in length ( $n = 719$ ) from an outside-out patch in the presence of  $1\ \mu\text{M}$  ATP. Membrane potential,  $-60\ \text{mV}$ . The shut time distribution is plotted with the log of the shut time on the ordinate versus the square root of the bin frequency on the abscissa (Sigworth & Sine, 1987; McManus *et al.* 1987). This transformation converts the normal exponential distribution into a peaked distribution and each peak corresponds to the time constant of each exponential component. The distribution was best fitted with the sum of five exponential components, with means (and relative areas) of  $56\ \mu\text{s}$  ( $21\%$ ),  $0.84\ \text{ms}$  ( $50\%$ ),  $19.0\ \text{ms}$  ( $6\%$ ),  $1185\ \text{ms}$  ( $12\%$ ) and  $5367\ \text{ms}$  ( $11\%$ ). The mean shut time was  $716\ \text{ms}$ . The fit predicts the existence of 889 gaps. *B*, distribution of all shut times greater than  $68\ \mu\text{s}$  in duration ( $n = 1558$ ) from the same patch as illustrated in Fig. 1*A*, in the presence of  $1\ \text{mM}$  ATP at a membrane potential of  $-60\ \text{mV}$ . The distribution was best fitted with the sum of five exponential components, with means (and relative areas) of  $30\ \mu\text{s}$  ( $38\%$ ),  $0.25\ \text{ms}$  ( $11\%$ ),  $1.3\ \text{ms}$  ( $14\%$ ),  $24\ \text{ms}$  ( $22\%$ ) and  $147\ \text{ms}$  ( $14\%$ ). The mean shut time was  $31\ \text{ms}$ . The fit predicts the existence of 2289 gaps. *C*, the effect of increasing ATP concentration on the mean shut time. Data are expressed as means  $\pm$  s.e.m. from four patches at  $1$  and  $40\ \mu\text{M}$  ATP, and 15 patches at  $1\ \text{mM}$  ATP. *D*, effect of increasing ATP concentration on the time constants of the shut time distribution. Data for each component are expressed as means  $\pm$  s.e.m. from four patches at  $1$  and  $40\ \mu\text{M}$  ATP, and 15 patches at  $1\ \text{mM}$  ATP. ■, time constant of the first (fastest) exponential; ▲ and ▼, second and third time constants of the shut time distribution, respectively; ◆, time constant of the fourth exponential; ●, time constant of the fifth component. *E*, effect of increasing ATP concentration on the relative areas of the exponential components of the shut time distribution. Data points representing the relative area of each exponential component of the shut time distribution are expressed as means  $\pm$  s.e.m. from four patches at  $1$  and  $40\ \mu\text{M}$  ATP, and 15 patches at  $1\ \text{mM}$  ATP. ■, relative area of the first (fastest) exponential; ▲ and ▼, relative area of the second and third exponential components, respectively; ◆, relative area of the fourth exponential; ●, relative area of the fifth component.

time constant did not significantly decrease between  $1 \mu\text{M}$  and  $1 \text{ mM}$  ATP ( $P = 0.08$ ). Intriguingly, there was a significant decrease in the relative area of the second exponential component, and a concomitant increase in the relative area of the third exponential (Fig. 3E) with increasing ATP concentration (Student's  $t$  test;  $P < 0.05$ ). The time constants of the last two components of the shut time distribution did vary widely between patches at the same ATP concentration and decreased significantly as the ATP concentration was increased (Fig. 3D). These results overall suggest that components four and five of the shut time distribution represent closed states that involve agonist binding to the receptor.

**Distribution of apparent open times.** The presence of a partially resolved fast exponential component in the shut time distributions suggests that many openings will in fact contain unresolved short gaps. Openings are therefore referred to as 'apparent' openings here. Distributions of apparent open times were best fitted with two exponential components (Fig. 4A and B). Figure 4A illustrates a typical open time distribution for a patch held at  $-60 \text{ mV}$  in the presence of  $1 \mu\text{M}$  ATP, which is qualitatively similar to the distribution observed in the presence of  $1 \text{ mM}$  ATP (Fig. 4B). There was a significant (unpaired  $t$  test;  $P > 0.05$ ) increase in mean open time on increasing the ATP concentration from  $1 \mu\text{M}$  to  $1 \text{ mM}$  (Fig. 4C). There was no evidence that the

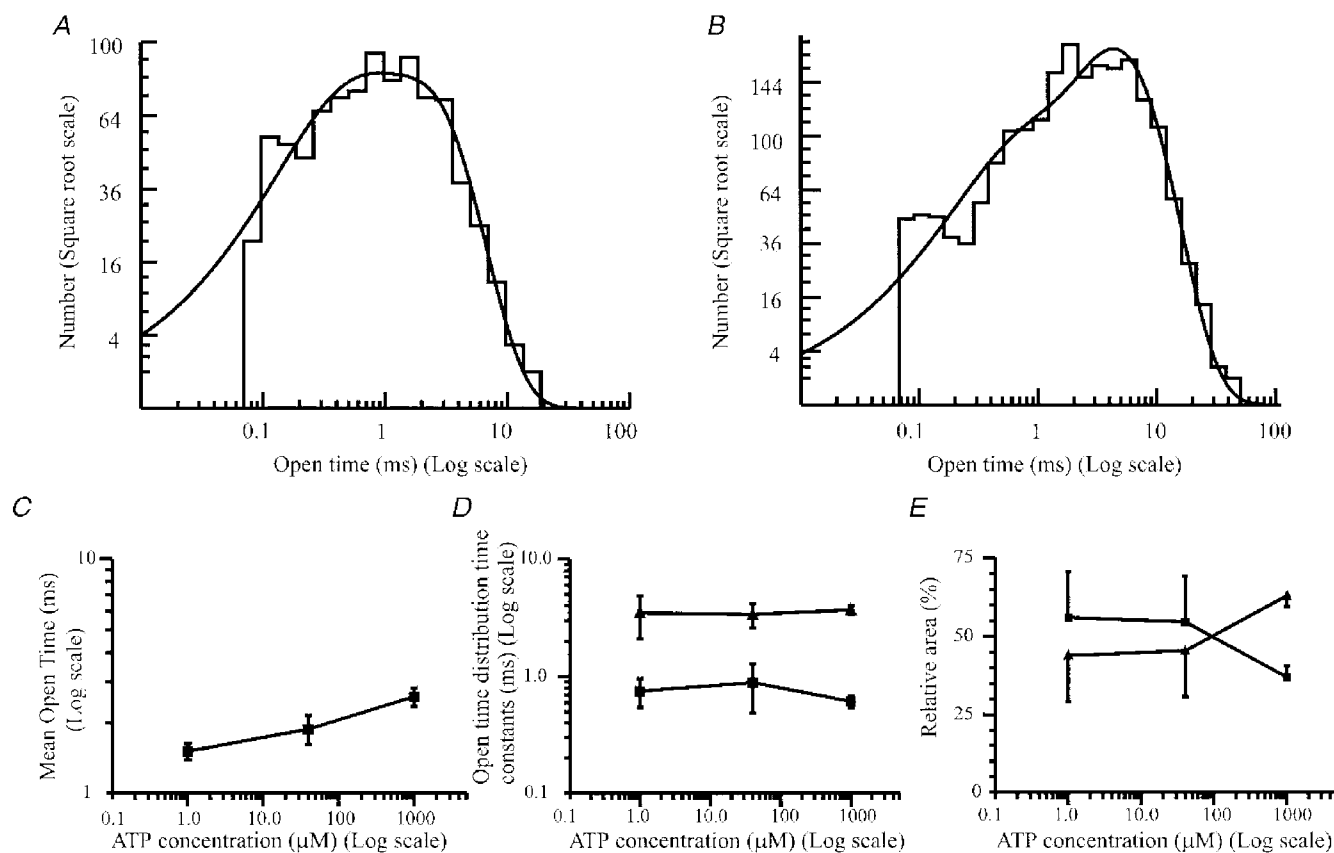


**Figure 4.** Agonist concentration dependence of P2X receptor open times

*A*, distribution of 876 apparent open times between  $70 \mu\text{s}$  and  $30 \text{ ms}$  in the presence of  $1 \mu\text{M}$  ATP. Membrane potential,  $-60 \text{ mV}$ . The data were best fitted with two exponential components. These had time constants (and relative areas) of  $0.35 \text{ ms}$  (33%) and  $1.8 \text{ ms}$  (67%). The mean open time was  $1.35 \text{ ms}$ , and the fit predicts that there were 956 apparent openings in the data record. *B*, distribution of the length of 2082 apparent open times between  $60 \mu\text{s}$  and  $50 \text{ ms}$  long from the patch shown in Fig. 1, in the presence of  $1 \text{ mM}$  ATP. The data were fitted with the sum of two exponential components with parameters of  $0.46 \text{ ms}$  (20%) and  $4.3 \text{ ms}$  (80%). The fit predicts that there were 2183 apparent openings in the data record with a mean open time of  $3.58 \text{ ms}$ . *C*, the effect of increasing ATP concentration on the mean channel open time. Data points show means  $\pm$  s.e.m. from at least four patches at each agonist concentration. *D*, the effect of changing ATP concentration on the components of the open time distribution. Data points show means  $\pm$  s.e.m. from at least four patches at each ATP concentration. ■, time constant of the first (fastest) component of the distribution; ▲, mean of the time constant of the second component. *E*, effect of increasing ATP concentration on the relative areas of the time constants of the open time distribution. Data points representing the relative area of each exponential component of the open time distribution show the mean  $\pm$  s.e.m. from four patches at  $1$  and  $40 \mu\text{M}$  ATP, and 15 patches at  $1 \text{ mM}$  ATP. ■, relative area of the first (fastest) exponential; ▲, relative area of the second component of the open time distribution.

exponential time constants of the open time distributions were dependent upon agonist concentration (Fig. 4D). The data indicate that there was a decrease in the relative area of the first exponential component with increasing ATP concentration (Fig. 4E). There was a concomitant increase in the relative area of the second component with increasing agonist concentration (Fig. 4E).

**Burst length distribution.** Bursts were defined as groups of openings separated by shut times which were shorter than a critical gap length,  $t_{\text{crit}}$ . The value of  $t_{\text{crit}}$  was calculated to lie between  $\tau_2$  and  $\tau_3$ , the second and third components of the shut time distribution. However, this

definition of  $t_{\text{crit}}$  is imperfect, as the tenfold difference between the time constants of these two components is not large enough to unambiguously classify shut times as 'between bursts' or 'within bursts'. The mean  $t_{\text{crit}}$  used to construct burst length distributions was not significantly dependent on ATP concentration (Student's  $t$  test;  $P > 0.05$ ) and was  $2.2 \pm 0.35$  ms at 1 mM ATP,  $2.2 \pm 0.16$  ms at  $40 \mu\text{M}$  ATP and  $2.8 \pm 0.27$  ms at  $1 \mu\text{M}$  ATP. Burst length distributions, as shown in Fig. 5A and B were constructed and were best fitted with the sum of three exponential components. There was no clear indication that the exponential components of the burst length distributions

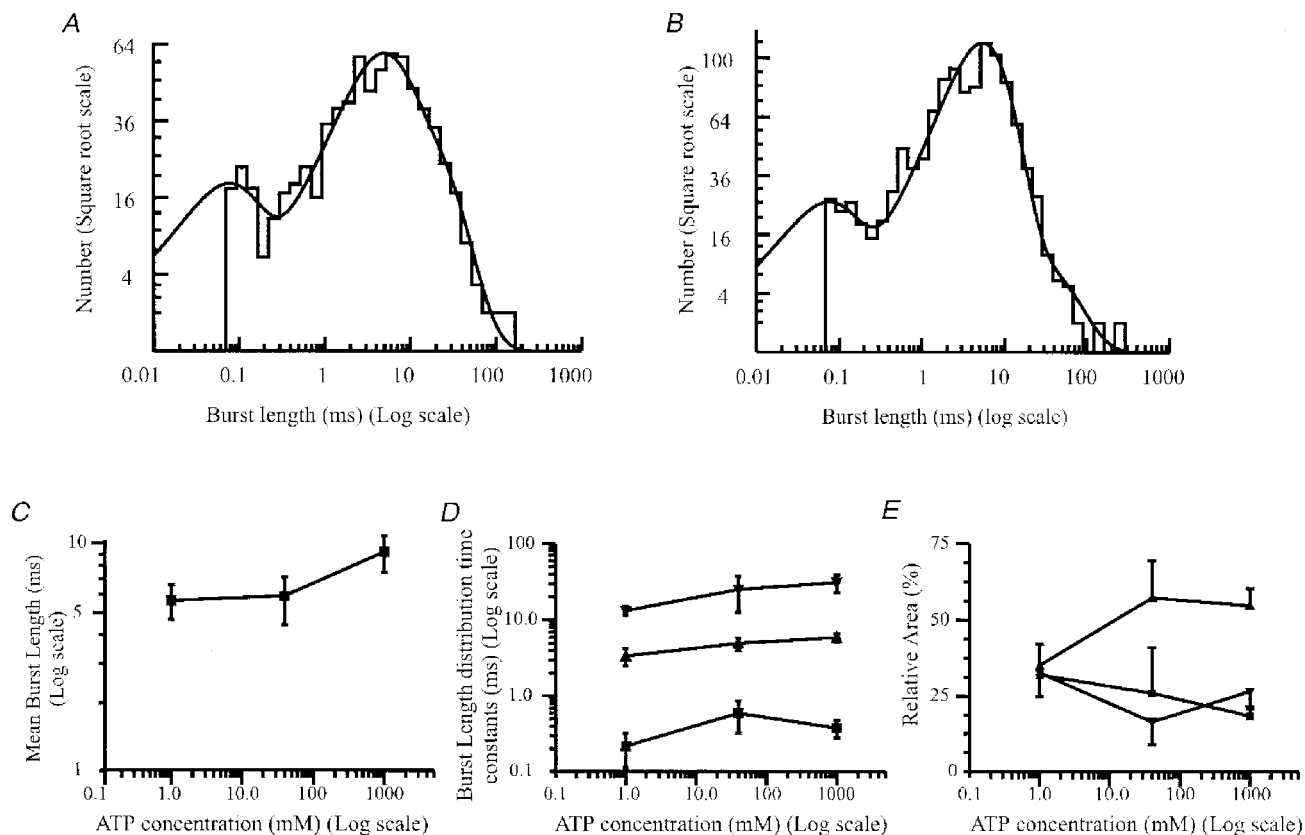


**Figure 5.** P2X receptor burst length properties

A, distribution of burst lengths for an outside-out patch exposed to  $1 \mu\text{M}$  ATP. The critical gap length ( $t_{\text{crit}}$ ) was  $2.03$  ms and 726 bursts were identified between  $70 \mu\text{s}$  and  $130$  ms long. The distribution was best fitted with the sum of three exponential components with time constants (and relative areas) of  $0.13$  ms (12%),  $4.0$  ms (53%) and  $14$  ms (35%). The distribution mean gave a mean burst length of  $7.18$  ms and a total of 737 bursts. B, distribution of burst lengths for the same patch as in Fig. 1A, in the presence of  $1$  mM ATP. The critical gap length was  $0.42$  ms and 1143 bursts were identified between  $69 \mu\text{s}$  and  $247$  ms long. The distribution is shown fitted with the sum of three exponential components, with parameters of  $60 \mu\text{s}$  (16%),  $5.2$  ms (78%) and  $25$  ms (6%). The fitted curve predicts a mean burst length of  $5.6$  ms and a total of 1169 bursts. C, the effect of increasing ATP concentration on the mean burst length. Data points represent the mean  $\pm$  s.e.m. burst length calculated from the time constants and relative areas of each individual component from at least four patches at each ATP concentration. D, the effect of ATP concentration on the burst distribution exponential time constants. ■, first component; ▲ and ▼, second and third components of the burst length distribution, respectively. E, effect of increasing ATP concentration on the relative areas of the time constants of the burst length distribution. Data points representing the relative area of each exponential component of the burst length distribution show the mean  $\pm$  s.e.m. from four patches at  $1$  and  $40 \mu\text{M}$  ATP, and 15 patches at  $1$  mM ATP. ■, relative area of the first (fastest) exponential component; ▲ and ▼, relative area of the second and third components, respectively.



were dependent on ATP concentration (Fig. 5). There was a slight increase in the mean burst length of the receptor with increasing agonist concentration (Fig. 5C), from  $5.4 \pm 0.9$  ms in  $1 \mu\text{M}$  ATP to  $8.8 \pm 1.8$  ms in  $1 \text{ mM}$  ATP. The mean burst length was  $5.63 \pm 1.3$  ms in  $40 \mu\text{M}$  ATP.

**Distribution of the total open time per burst.** In principle, the number of components in the distribution of total open time per burst should equal the number of components in the open time distribution, and is a measure of the number of open states that the receptor can exist in (Colquhoun & Hawkes, 1981, 1982). Distributions of the total open time per burst (Fig. 6A and B) were fitted with three exponential components. Both the time constants and

the relative areas of these three components were very similar to those obtained for the burst length distributions, as expected for bursts where the gaps within bursts are relatively short.

The fraction of time for which the channel is open during a particular burst (i.e. the burst  $P_{\text{open}}$ ) was calculated by dividing the mean total open time per burst by the mean burst length. At  $-60$  mV the mean burst  $P_{\text{open}}$  was  $0.96 \pm 0.03$  for the 15 patches in the presence of  $1 \text{ mM}$  ATP, and for the four patches with different ATP concentrations this was  $0.79 \pm 0.02$  at  $1 \mu\text{M}$  ATP,  $0.89 \pm 0.02$  at  $40 \mu\text{M}$  ATP, and  $0.94 \pm 0.03$  at  $1 \text{ mM}$  ATP. Thus, ATP activates hippocampal P2X receptors with high efficacy when the

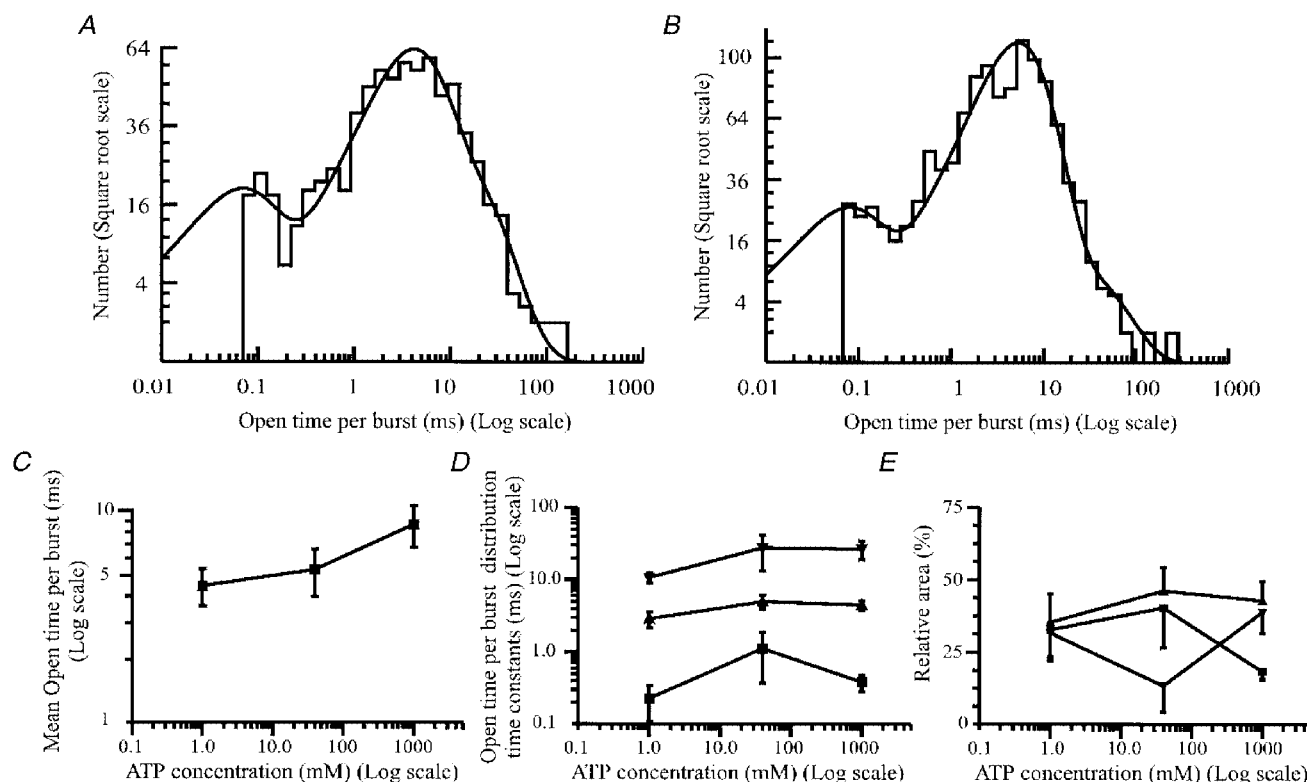


**Figure 6.** P2X receptor total open time per burst

*A*, distribution of the total open time per burst from the same patch as shown in Fig. 5A in the presence of  $1 \mu\text{M}$  ATP. The distribution includes 726 bursts between  $70 \mu\text{s}$  and  $120$  ms long and was best fitted with the sum of three exponential components with time constants (and relative areas) of  $60 \mu\text{s}$  (19%),  $3.6$  ms (57%) and  $14$  ms (24%). The mean total open time per burst was  $5.97$  ms and the fit predicted the existence of 735 individual open times. *B*, distribution of the total open time per burst from the same patch as shown in Fig. 5B in the presence of  $1 \text{ mM}$  ATP. The distribution includes 1143 bursts and was best fitted with the sum of three exponential components. These had time constants (and relative areas) of  $66 \mu\text{s}$  (16%),  $5.2$  ms (78%) and  $25$  ms (6%). The distribution mean was calculated to be  $5.5$  ms. The fit predicts 1290 individual open times. *C*, effect of increasing ATP concentration on the mean total open time per burst of the channel. Data points are means  $\pm$  s.e.m. from four patches at  $1$  and  $40 \mu\text{M}$  ATP, and 15 patches at  $1 \text{ mM}$  ATP. *D*, the effect of increasing ATP concentration on the open time per burst time constants. ■, time constant of the first (fastest) exponential component of the distribution; ▲ and ▼, time constants of components two and three of the distribution, respectively. Data points are means  $\pm$  s.e.m. from four patches at  $1$  and  $40 \mu\text{M}$  ATP, and 15 patches at  $1 \text{ mM}$  ATP. *E*, effect of increasing ATP concentration on the relative areas of the time constants of the open time distribution. Data representing the relative area of each exponential component of the open time per burst distribution are expressed as means  $\pm$  s.e.m. from four patches at  $1$  and  $40 \mu\text{M}$  ATP, and 15 patches at  $1 \text{ mM}$  ATP. ■, relative area of the first (fastest) exponential; ▲ and ▼, relative area of the second and third components, respectively.

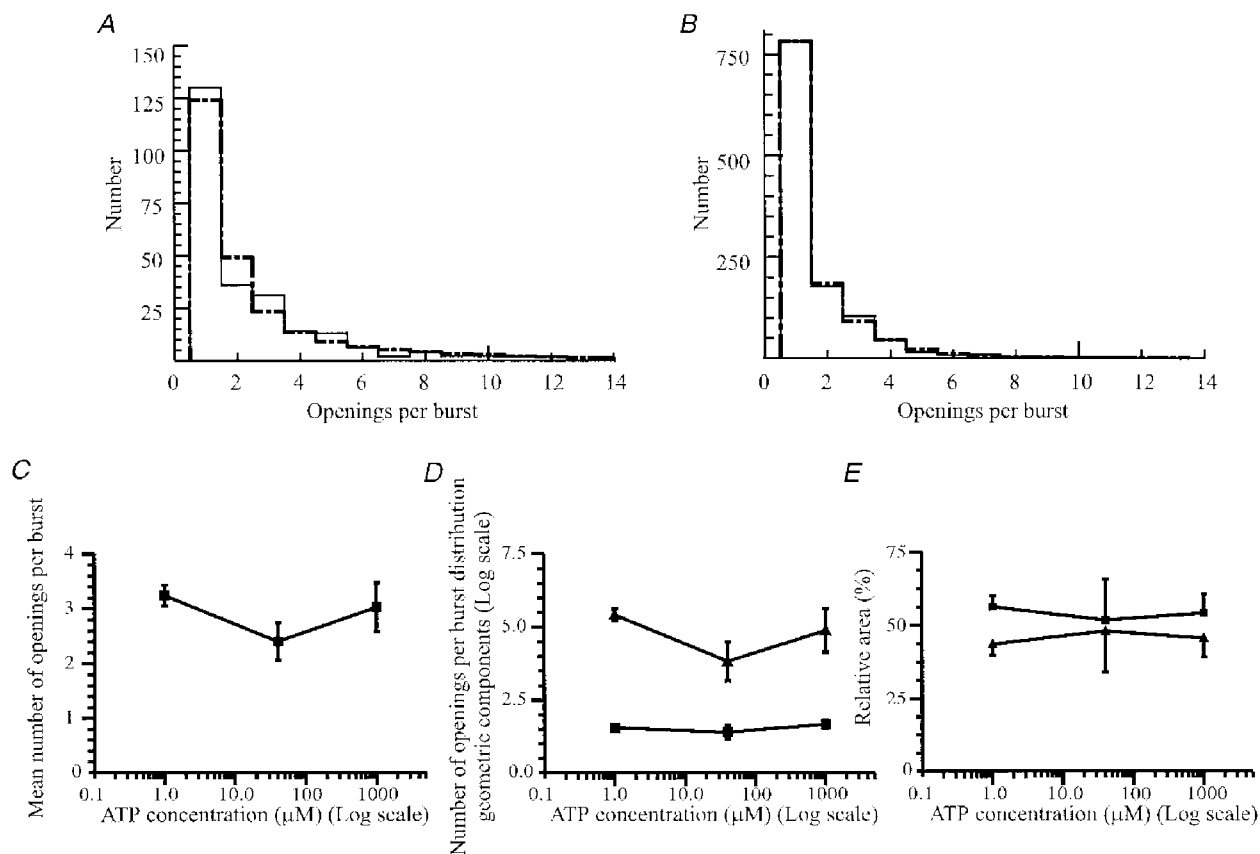
effects of desensitisation and agonist binding and unbinding are excluded.

**Distribution of the number of apparent openings per burst.** In principle, since there are three exponential components in the total open time per burst distribution, there should be three geometric components in distributions of the number of openings per burst and three exponential components in distributions of apparent open times (Colquhoun & Hawkes, 1981, 1982). However, as with the dwell time distributions, some of the components may be missed if they are too small to be detected or have a mean near to that of another component. In these experiments, we detected only two geometric components in distributions

of the number of openings per burst (Fig. 7*A* and *B*, Table 1). There was no evidence of any agonist concentration dependence of the number of openings per burst (Fig. 7*C*, *D* and *E*).

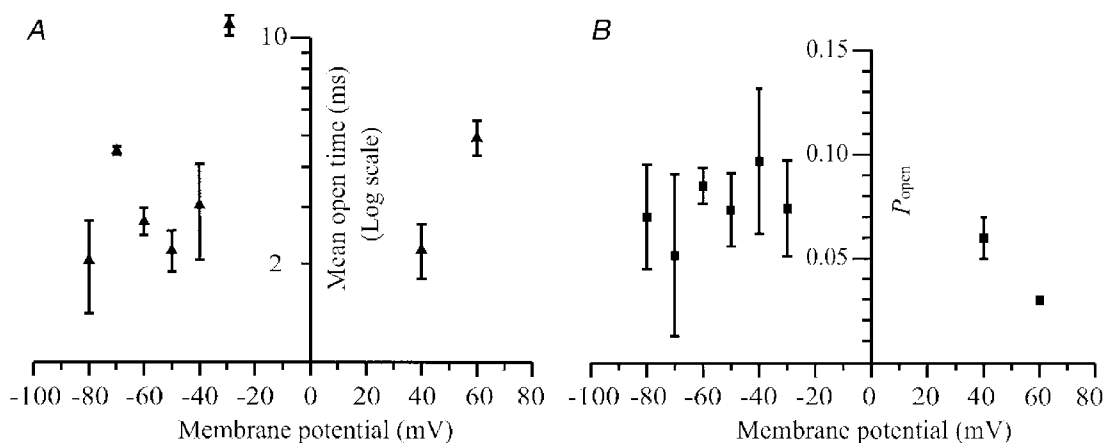
#### Voltage dependence of large conductance P2X receptor properties

Figure 8*A* shows that there is at most only a slight voltage dependence of the mean open time and no obvious voltage dependence of the overall  $P_{\text{open}}$  of the large conductance P2X receptor. Unlike the P2X receptors observed in superior cervical ganglia (Cloues, 1995), the hippocampal large conductance P2X receptor shows a significant (linear regression  $F$  test,  $P < 0.05$ ) voltage-dependent increase in



**Figure 7.** P2X receptor number of openings per burst

*A*, distribution of the number of openings per burst elicited by 1 μM ATP. The distribution was fitted with the sum of two geometric components with means (and relative areas) of 1.8 (55%) and 5.1 (45%) openings per burst. The fitted geometric components are represented as dashed lines superimposed on the distribution. The distribution mean was 3.3 openings per burst. *B*, distribution of the number of apparent openings per burst fitted with two geometric components from a patch in the presence of 1 mM ATP. The components of the fit had means (and relative areas) of 1.0 (35%) and 2.0 (65%) openings per burst. The mean for this distribution averaged 1.6 openings per burst. *C*, the effect of increasing ATP concentration on the mean number of openings per burst from at least four patches at each ATP concentration. *D*, the effect of ATP concentration on the mean of each geometric component in distributions of the number of openings per burst; ■, first component; ▲, second component. *E*, effect of increasing ATP concentration on the relative areas of the time constants of the number of openings per burst distribution. Data points representing the relative area of each geometric component of the number of openings per burst distribution are expressed as means  $\pm$  s.e.m. from four patches at 1 and 40 μM ATP, and 15 patches at 1 mM ATP. ■, relative area of the first geometric component; ▲, relative area of the second component. Data points are connected by a straight line drawn through the data obtained for the relative area of each separate component.



**Figure 8. Voltage dependence of P2X receptor open times and  $P_{open}$**   
 The data points represent means  $\pm$  s.e.m. for 3–5 patches at each voltage of the mean open time (A) and  $P_{open}$  (B).

the burst length and mean total open time per burst with depolarisation (Fig. 9A and B). This is due to the voltage-dependent increase in the number of apparent openings per burst (Fig. 9C). There was no evidence of any voltage dependence of the open probability per burst, as shown in Fig. 9D.

**The effect of suramin on the large conductance P2X receptor**

Suramin is the drug most widely used to antagonise P2X receptors. A feature of homomeric P2X<sub>4</sub> and P2X<sub>6</sub> receptor channels is that they are not antagonised by suramin (Bo *et al.* 1995; Collo *et al.* 1996; but see Séguéla *et al.* 1996),

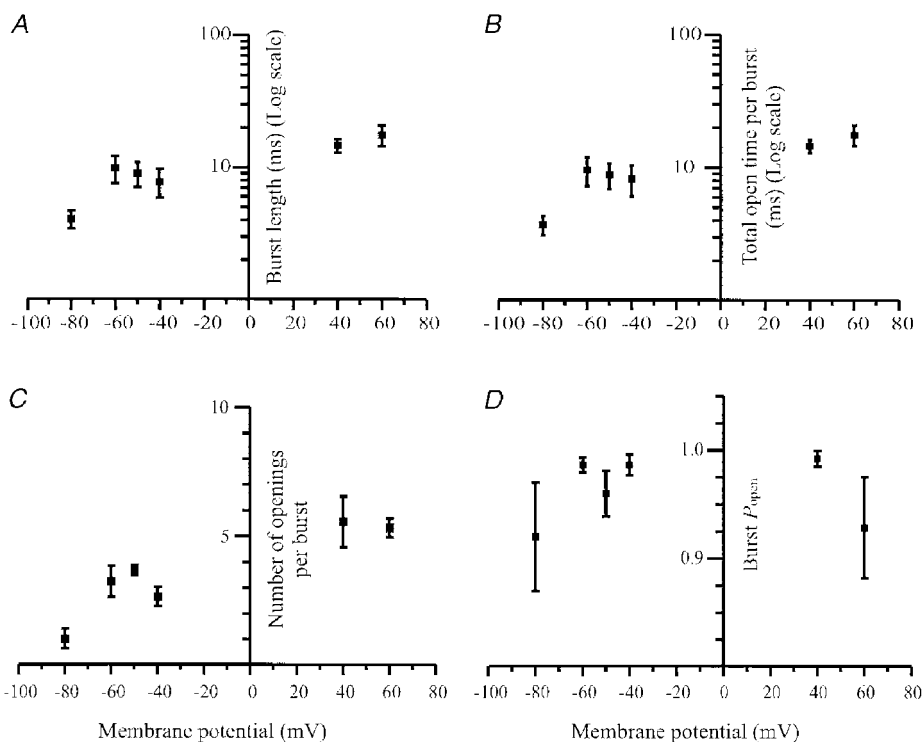


**Figure 9. Relationship between single channel burst parameters and membrane potential**  
 Data are from three to five patches at each membrane potential. In each graph data points represent means  $\pm$  s.e.m. of the burst parameters calculated from fits to the burst distributions obtained at each membrane potential. The slope of the linear regression line in each graph was significantly different from zero ( $P > 0.05$ ), apart from the burst  $P_{open}$  which was not significantly voltage dependent ( $P = 0.98$ ). A, voltage dependence of burst lengths. B, voltage dependence of mean total open time per burst. C, voltage dependence of the number of apparent openings per burst. D, voltage dependence of  $P_{open}$  during a burst.

whereas homomeric receptors formed by the expression of other P2X receptor subtypes are sensitive to suramin. Figure 10 shows qualitatively the effect of suramin at the single channel level. The figure illustrates that 40  $\mu\text{M}$  suramin, a concentration which should block responses mediated by homomeric P2X<sub>1</sub>, P2X<sub>2</sub>, P2X<sub>3</sub> or P2X<sub>5</sub> receptors, leads to a reduction in the frequency of openings and an increase in the closed periods between channel openings. In order to avoid possible rundown of channel activity being interpreted as inhibition by suramin, control periods of recording in the presence of 1 mM ATP were made both before and after application of 1 mM ATP in the presence of 40  $\mu\text{M}$  suramin. The effect of suramin was expressed relative to the mean activity measured before and after suramin application. Suramin significantly increased the single channel conductance of these receptors by  $19 \pm 7\%$  ( $P < 0.05$ ) from  $52 \pm 1.8$  pS to  $62 \pm 3.3$  pS. A similar effect of suramin could account for part of the 33% increase in homomeric P2X<sub>4</sub> whole-cell current seen in the presence of suramin (Bo *et al.* 1995). This increase in single channel conductance in the presence of suramin indicates that the action of suramin is not competitive at these receptors. In four out of five patches, suramin produced a significant decrease ( $46 \pm 11\%$ ;  $P < 0.05$ ) in  $P_{\text{open}}$  from  $0.064 \pm 0.016$  to  $0.032 \pm 0.005$ . However, in one patch,  $P_{\text{open}}$  increased from 0.048 to 0.06. When the data obtained from this other patch were taken into account, a significant decrease in  $P_{\text{open}}$  of the hippocampal P2X receptor ( $30 \pm 16\%$ ) and a significant decrease in mean open time ( $27 \pm 9\%$ ) occurred in the presence of suramin. In addition,

40  $\mu\text{M}$  suramin caused a significant decrease in the mean burst length ( $31 \pm 13\%$ ), suggesting that the main effect of suramin is to reduce the duration of P2X receptor activation.

#### Large conductance channels activated by $\alpha,\beta$ -meATP

The synthetic purinoceptor agonist  $\alpha,\beta$ -meATP (40  $\mu\text{M}$ ) also activated large conductance channels in 3 out of 17 outside-out patches from granule cells, with a chord conductance of  $57 \pm 1.1$  pS at  $-60$  mV. The mean open time of these receptors was  $6.2 \pm 1.2$  ms with a mean shut time of  $652 \pm 197$  ms. This compares with a conductance of  $56 \pm 1.8$  pS and mean open time of  $1.8 \pm 0.27$  ms for channels activated by 40  $\mu\text{M}$  ATP.

#### Flickery P2X receptors

In addition to the large conductance P2X receptor, a P2X receptor with more stereotypical flickery openings was also observed in dentate gyrus granule cells. However, this was observed in only three patches, and the receptor appeared to desensitise in the continued presence of ATP. A 2 s recording of the flickery channel at a membrane potential of  $-60$  mV is illustrated in Fig. 11A. There are a number of qualitative differences between the channels observed in this trace and those illustrated in Fig. 1. Firstly, there are at least three active channels in the patch and the channel activations occur in long bursts. It can also be seen that the channel flickers rapidly between open and shut states. Figure 11B shows the open–shut point amplitude distribution for the patch shown in Fig. 11A. The distribution in Fig. 11B was best fitted with three Gaussian

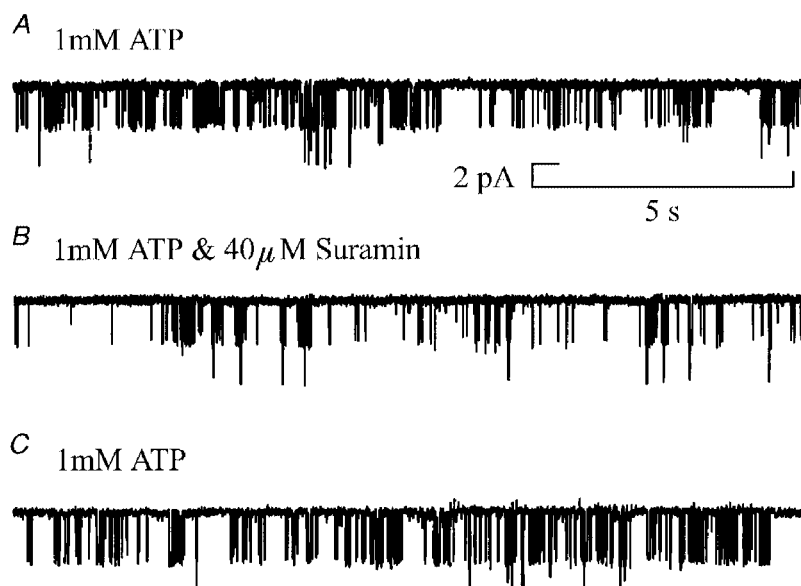


**Figure 10.** The effect of 40  $\mu\text{M}$  suramin on single channel currents activated by 1 mM ATP

Outside-out patch. Membrane potential,  $-60$  mV. Channel openings are shown as downward deflections from the baseline. Each horizontal trace shows a 15 s recording before suramin addition (upper trace;  $P_{\text{open}} = 0.095$ ), in the presence of ATP and suramin (middle trace;  $P_{\text{open}} = 0.038$ ), and following suramin washout (lower trace;  $P_{\text{open}} = 0.053$ ) to demonstrate the pattern of channel activity. Currents were low-pass filtered at 2 kHz ( $-3$  dB) and sampled at 20 kHz.

components, implying that a subconductance level is present, although there was no evidence of this from the amplitude distributions obtained from the other two patches, which were fitted with the sum of two Gaussian components (closed channel level and one open level). We conclude that, like the large conductance P2X receptor, the flickery channel exhibits only one main conductance level of  $1.89 \pm 0.3$  pA at  $-60$  mV, which corresponds to a chord conductance of  $32 \pm 6$  pS, assuming a linear current–voltage relationship and a reversal potential of 0 mV.

The shut time histograms for the flickery P2X receptors, while fitted with the same number of components (five) as those obtained for the large conductance P2X receptor, were qualitatively and quantitatively very different (compare Fig. 11C with Fig. 3A and B). The five exponentials had time

constants (and relative areas) of  $\tau_1 = 51 \pm 0.6$   $\mu$ s ( $36 \pm 23\%$ ),  $\tau_2 = 0.59 \pm 0.21$  ms ( $23 \pm 11\%$ ),  $\tau_3 = 1.06 \pm 0.25$  ms ( $30 \pm 10\%$ ),  $\tau_4 = 20.1 \pm 6.37$  ms ( $4.5 \pm 2.0\%$ ) and  $\tau_5 = 1682 \pm 1440$  ms ( $6.4 \pm 4.6\%$ ). The distribution mean was  $23 \pm 6.8$  ms. The open time distributions were also very different from those of the large conductance channel (compare Fig. 11D with Fig. 4A and B), and were best fitted with the sum of three exponential components, in contrast to open time histograms for the large conductance P2X receptor which were best fitted with two exponentials. The open time distributions for the flickery channel had time constants (and relative areas) of  $\tau_1 = 0.38 \pm 0.11$  ms ( $29 \pm 23\%$ ),  $\tau_2 = 1.2 \pm 0.45$  ms ( $33 \pm 21\%$ ) and  $\tau_3 = 3.3 \pm 1.6$  ms ( $38 \pm 30\%$ ). The mean apparent open time of these flickery channels was  $0.98 \pm 0.27$  ms.

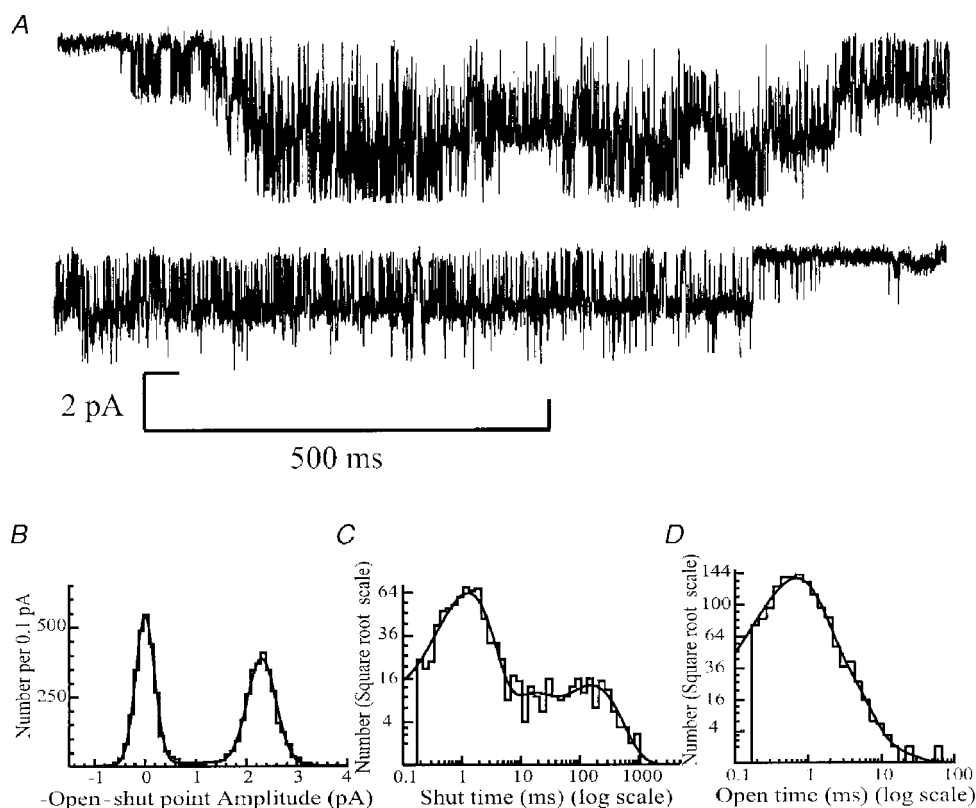


**Figure 11. Flickery single channel currents activated by 1 mM ATP**

Outside-out patch. Membrane potential,  $-60$  mV. Multiple flickery channel openings are illustrated as downward deflections from the baseline. The traces show two contiguous sweeps of 1.1 s duration demonstrating the flickery nature of this single channel behaviour. Currents were low-pass filtered at 2 kHz ( $-3$  dB) and sampled at 20 kHz. *B*, open–shut point amplitude distribution of 1175 open and closed periods of longer than two filter rise times ( $t_r = 0.332$  ms). The distribution was fitted with the sum of three Gaussian components with fitted parameters of 0.003 pA (relative area, 45%; s.d. = 0.19 pA), 1.28 pA (7%; s.d. = 1.25 pA) and 2.30 pA (48%; s.d. = 0.28 pA), giving a mean single channel amplitude of 2.17 pA and open probability of 0.55. *C*, distribution of the length of 887 shut times longer than 170  $\mu$ s in duration. The distribution was best fitted with the sum of five exponential components with parameters of 50  $\mu$ s (relative area, 6%), 0.9 ms (26%), 1.5 ms (44%), 12 ms (8%) and 154 ms (16%). The mean shut time was 26 ms. The fit predicts the existence of 1044 shut times. *D*, distribution of the length of 1417 apparent open times longer than 170  $\mu$ s in duration. The data were fitted with the sum of three exponential components with time constants (and relative areas) of 0.6 ms (74%), 2 ms (25%) and 6 ms (1%). The mean apparent open time was 1 ms. The fit predicts that there were 1779 openings in the data record.

Table 1. Summary of distribution parameters for large conductance hippocampal P2X receptors

Component	1 ( $\mu$ s)	2 (ms)	3 (ms)	4 (ms)	5 (ms)	Distribution mean
Apparent open time	—	$0.7 \pm 0.06$	$3.7 \pm 0.3$	—	—	$2.6 \pm 0.24$ ms
Relative area	—	$37 \pm 4\%$	$63 \pm 4\%$	—	—	
Shut time	$90 \pm 10$	$0.76 \pm 0.09$	$10 \pm 2.1$	$90 \pm 24$	$403 \pm 103$	$62 \pm 10$ ms
Relative area	$20 \pm 2\%$	$32 \pm 4\%$	$15 \pm 2\%$	$18 \pm 3\%$	$15 \pm 2\%$	
Burst length	—	$0.38 \pm 0.09$	$5.9 \pm 0.8$	$31 \pm 8$	—	$8.8 \pm 1.8$ ms
Relative area	—	$19 \pm 3\%$	$55 \pm 6\%$	$26 \pm 6\%$	—	
Total open time per burst	—	$0.38 \pm 0.09$	$4.9 \pm 0.6$	$42 \pm 15$	—	$8.4 \pm 1.8$ ms
Relative area	—	$19 \pm 3\%$	$46 \pm 7\%$	$35 \pm 8\%$	—	
No. of openings per burst	$1.7 \pm 0.15$	$4.9 \pm 0.7$	—	—	—	$3.0 \pm 0.44$
Relative area	$54 \pm 6\%$	$46 \pm 6\%$	—	—	—	
Burst $P_{\text{open}}$	—	—	—	—	—	$0.96 \pm 0.03$

Measurements of the distribution parameters obtained from the analysis of P2X receptor channel activity in the presence of 1 mM ATP at  $-60$  mV ( $n = 15$ ). Shown is the mean  $\pm$  s.e.m. of each parameter, and immediately below each parameter estimate is the mean  $\pm$  s.e.m. of the percentage area of that particular component.

Table 2. Summary of distribution parameters for flickery P2X receptors

Component	1 ( $\mu$ s)	2 (ms)	3 (ms)	4 (ms)	5 (ms)	Distribution mean
Apparent open time	—	$0.38 \pm 0.11$	$1.2 \pm 0.45$	$3.3 \pm 1.6$	—	$1.0 \pm 0.3$ ms
Relative area	—	$29 \pm 23\%$	$33 \pm 21\%$	$37 \pm 30\%$	—	
Shut time	$51 \pm 0.6$	$0.58 \pm 0.21$	$1.1 \pm 0.25$	$20 \pm 6.4$	$1682 \pm 1440$	$23 \pm 6.8$ ms
Relative area	$35 \pm 23\%$	$22 \pm 11\%$	$30 \pm 9\%$	$4 \pm 2\%$	$6 \pm 5\%$	
Burst length	—	$0.40 \pm 0.10$	$4.4 \pm 2.2$	$31 \pm 9.7$	—	$11 \pm 4.7$ ms
Relative area	—	$42 \pm 9\%$	$27 \pm 9\%$	$30 \pm 6\%$	—	
Total open time per burst	—	$0.48 \pm 0.07$	$6.8 \pm 2.3$	$30 \pm 8.3$	—	$9.5 \pm 4.9$ ms
Relative area	—	$47 \pm 12\%$	$35 \pm 4\%$	$18 \pm 10\%$	—	
No. of openings per burst	$1.2 \pm 0.14$	$19.8 \pm 3.0$	—	—	—	$9.0 \pm 1.2$
Relative area	$56 \pm 10\%$	$44 \pm 10\%$	—	—	—	
Burst $P_{\text{open}}$	—	—	—	—	—	$0.82 \pm 0.07$

Measurements of the distribution parameters obtained from the analysis of P2X receptor channel activity in the presence of 1 mM ATP at  $-60$  mV ( $n = 3$ ). Shown is the mean  $\pm$  s.e.m. of each parameter, and immediately below each parameter estimate is the mean  $\pm$  s.e.m. of the percentage area of that particular component.

### The burst kinetics of flickery P2X receptors

Bursts were again defined to include all shut times which were shorter than a critical gap length,  $t_{\text{crit}}$ . The value of  $t_{\text{crit}}$  was calculated between the third and fourth components of the shut time distribution, as there was a twentyfold difference between these two components. The mean  $t_{\text{crit}}$  that was used for the analysis of bursts was  $2.1 \pm 0.49$  ms. Burst length distributions were fitted with the sum of three exponential components, with time constants (and relative areas) of  $\tau_1 = 0.41 \pm 0.10$  ms ( $43 \pm 9\%$ ),  $\tau_2 = 4.3 \pm 2.2$  ms ( $27 \pm 9\%$ ) and  $\tau_3 = 31 \pm 9.7$  ms ( $30 \pm 6\%$ ). The distribution means gave a mean burst length of  $11 \pm 4.7$  ms (Table 2).

Distributions of total open time per burst were also fitted with the sum of three exponentials. The time constants (and relative areas) of the distributions were  $\tau_1 = 0.48 \pm 0.06$  ms ( $47 \pm 12\%$ ),  $\tau_2 = 6.8 \pm 2.3$  ms ( $35 \pm 4\%$ ) and  $\tau_3 = 30 \pm 8.3$  ms ( $18 \pm 10\%$ ), with a distribution mean of  $9.55 \pm 4.9$  ms. The burst  $P_{\text{open}}$  for the flickery channel was  $0.82 \pm 0.07$  (Table 2).

Distributions of the number of apparent openings per burst were best fitted with the sum of two geometric components. These had values of  $1.4 \pm 0.14$  ( $55 \pm 10\%$ ) and  $20 \pm 2.9$  ( $44 \pm 10\%$ ), respectively. The mean number of openings per burst was  $9.04 \pm 1.23$  (Table 2).

## DISCUSSION

The results presented here provide the first description of the single channel properties of native P2X receptors from dentate gyrus granule cells in rat hippocampal slices. Hippocampal P2X receptor channel openings occur in bursts and the properties of these bursts (short openings, short gaps and a high  $P_{\text{open}}$  within the burst) are consistent with the general principles of ligand-gated ion channel receptor activation, as first described for the muscle nicotinic ACh receptor (Colquhoun & Sakmann, 1985). This is an interesting observation, given that the protein structure of P2X receptors is likely to be quite different from that of nicotinic or other ion channel receptors (Brake *et al.* 1994; Valera *et al.* 1994). The activation properties of hippocampal P2X receptors are also consistent with a physiological role of mediating fast excitatory synaptic transmission (Edmonds *et al.* 1995). We have also demonstrated the existence of two distinct populations of P2X receptor in hippocampal granule cells, which are referred to here as the large conductance P2X receptor and the flickery P2X receptor. Both species of P2X receptor have unique single channel characteristics when compared to other native and recombinant P2X receptors.

Despite the relatively high density of P2X receptor subunit mRNA (Collo *et al.* 1996) and protein (Kidd *et al.* 1995; Lê *et al.* 1998b) in the hippocampus, functional P2X receptors were only observed in a total of 22 out of 115 patches. Firstly, this may be because functional receptors are expressed at a low density, or they could be localised preferentially in the dendrites or axon terminals of the granule cell rather than at the cell body, from which membrane patches were isolated. However, in most patches where channel activity was observed, some double openings were present. These double openings occurred at a much higher frequency than would be expected if they were due to the random superposition of background channels evident in the absence of ATP with those channels activated by ATP application. This suggests that P2X receptors may be clustered in the cell membrane rather than exhibiting an even but sparse distribution over the soma. Secondly, it could be that the majority of P2X receptors on the granule cells are non-functional, but those that are functional exist in functional groups. A third reason for the lack of active P2X receptors in many outside-out patches could be that patch excision inactivates these P2X receptors.

### Single channel conductance

The results of this study show that both the large conductance (55 pS) and flickery (32 pS) P2X receptors in the hippocampus open to one main conductance level. The single channel conductance is larger than has previously been reported for homomeric P2X<sub>1</sub>, P2X<sub>2</sub>, P2X<sub>3</sub> or P2X<sub>4</sub> receptors expressed in CHO cells. Evans (1996) described flickery channels due to activation of homomeric P2X<sub>1</sub>, P2X<sub>2</sub> and P2X<sub>4</sub> receptors, with chord conductances at -100 mV of 18, 21 and 9 pS, respectively (in 0.3 mM extracellular calcium). Homomeric P2X<sub>3</sub> receptor channels

were reported to be too flickery to determine the single channel conductance accurately (Evans, 1996). P2X receptors with single channel conductances ranging from 0.2 to 63 pS have been observed in native tissue preparations, although it is necessary to consider a potential effect of calcium ions on conductance when comparing results from different studies. It has been demonstrated that raising the extracellular calcium concentration leads to a decrease in the single channel conductance of PC12 cell P2X receptors (Nakazawa & Hess, 1993), which are probably homomeric P2X<sub>2</sub> receptors (Brake *et al.* 1994), and the conductance of other cation channels, including NMDA receptors (Ascher & Nowak, 1988; Gibb & Colquhoun, 1992), and both endplate (Colquhoun & Sakmann, 1985) and ganglionic nicotinic ACh receptors, is sensitive to extracellular calcium (Mathie *et al.* 1991). However, the large conductance hippocampal P2X receptor was found in this study to have a slope conductance of 55 pS in both 0.3 and 0.85 mM free extracellular calcium. A conductance of 55 pS is much greater than that reported for recombinant homomeric P2X receptors (Evans, 1996; Zhou & Hume, 1998; Ding & Sachs, 1999) and greater than that of the majority of native P2X receptors, although a P2X receptor with a conductance of 63 pS has been observed in cardiac ganglia (Fieber & Adams, 1991). It is interesting to note that for P2X receptors expressed in sensory ganglia, when the calcium concentration is changed between 0.1 and 5 mM, the decrease in single channel conductance is relatively small (Krishtal *et al.* 1988), so not all P2X receptors have a calcium-sensitive single channel conductance like that described by Nakazawa & Hess (1993) for the P2X receptor in PC12 cells. It is possible that this property is related to channel calcium permeability and a number of studies have shown that both native and recombinant homomeric P2X receptors have significant calcium permeability (reviewed by Edwards *et al.* 1997).

The flickery channel in hippocampal granule cells had a single channel conductance of 31 pS in 0.3 mM calcium. This is close to the 35 pS observed by Krishtal *et al.* (1988) for a flickery P2X receptor channel in sensory ganglia (0.1 mM extracellular calcium). Further experiments need to be performed to determine whether changing the extracellular calcium concentration has any effect on the single channel properties of the hippocampal flickery P2X receptor.

The difference in single channel conductance between P2X receptors both within the hippocampus and between the hippocampus and other neuronal preparations (see e.g. Krishtal *et al.* 1988; Khakh *et al.* 1997) probably reflects differences in receptor subunit composition. P2X receptors are likely to be composed of either a trimer/hexamer (Nicke *et al.* 1998; Stoop *et al.* 1999) or a tetramer of subunits (Kim *et al.* 1997).

### Channel open times

The distribution of open times for the large conductance P2X receptor was best fitted with the sum of two exponential components, implying that the receptor can

exist in a minimum of two distinct open states. However, three components were necessary to fit distributions of the total open time per burst, suggesting that there are three open states (Colquhoun & Hawkes, 1982). A particular open state cannot be assigned to a particular conductance level, as two components were present in the open time distributions even when there was only a single component in the amplitude distribution. Therefore, these results suggest that the receptor is able to open to at least two discrete open states of 55 pS conductance. When the ATP concentration was lowered from 1 mM to 1  $\mu$ M, there was a decrease in the mean open time and a reduction in the percentage area of the slow exponential component of the open time distribution. This concentration dependence of the open time suggests that the open state of the receptor is dependent on the number of agonist molecules that are bound to the receptor. The distribution of open times for dorsal root ganglia P2X receptors has previously been shown to have two components (Krishtal *et al.* 1988) but their concentration dependence was not reported.

P2X receptors in sensory neurons have a Hill coefficient close to three suggesting that three agonist molecules need to bind to the receptor to produce efficient channel activation (Bean, 1990). However, studies of P2X receptors in vas deferens (Friel, 1988) and cardiac muscle (Friel & Bean, 1988) suggest that only two molecules of agonist need to bind to activate the receptor. Therefore, P2X receptors may exhibit two or three distinct open states dependent on the number of agonist molecules bound. Studies on nicotinic ACh receptors and GABA<sub>A</sub> receptors at low agonist concentrations suggest that a singly liganded channel can open briefly (Colquhoun & Sakmann, 1985; MacDonald *et al.* 1989*b*) but there was no evidence of this for NMDA receptors (Gibb & Colquhoun, 1992). A similar mechanism could underlie the shift in the relative area from the first to the second component of the open time distribution with increasing ATP concentration as the proportion of partially liganded receptors to fully liganded receptors will be higher at lower agonist concentrations.

### Channel closed times

The shut time distributions of both populations of P2X receptor were best fitted with the sum of five exponential components (Figs 3*A* and *B*, and 11*C*; Tables 1 and 2). The shut time distribution is therefore more complex than that of muscle nicotinic ACh receptors, which show only a short (20  $\mu$ s) component and a longer component of around 700 ms, with a small intermediate component (0.5 ms) (Colquhoun & Sakmann, 1985). In contrast to the nicotinic receptor, five exponential components are found in GABA<sub>A</sub>, glycine and NMDA receptor shut time distributions (MacDonald *et al.* 1989*b*; Twyman & Macdonald, 1991; Gibb & Colquhoun, 1992).

Both large conductance and flickery hippocampal P2X receptors can exist in at least five distinct shut states. As macroscopic current recordings suggest that either two

(Friel & Bean, 1988) or three (Bean, 1990) molecules of ATP can bind to other P2X receptors, then four of the five shut states could correspond to the free, monoliganded, doubly liganded and possibly triply liganded states of the receptor. Further shut states due to receptor desensitisation may be present, as desensitisation occurs with most native and recombinant P2X receptors (Valera *et al.* 1994; Brake *et al.* 1994; Chen *et al.* 1995; Bo *et al.* 1995; Collo *et al.* 1996). Precise physical correlates of the shut time components cannot be assigned without more detailed information about the mechanism of receptor activation. Since gaps between agonist binding events are likely to be very short at 1 mM ATP, the long gaps at this agonist concentration are more likely to represent periods when all receptors in the patch are desensitised. At low agonist concentrations, however, the long gaps are more likely to represent periods when all the receptors in the patch are unoccupied. The intriguing decrease in the relative area of the second exponential component of the shut time distribution (Fig. 3*E*) suggests that one of the open states occurs when the receptor is not fully liganded (Colquhoun & Hawkes, 1981), which is consistent with the concentration dependence of the open time distribution components illustrated in Fig. 4.

The fact that the time constants of the first two exponential components in the shut time distribution (for large conductance P2X receptors) are not dependent on the agonist concentration suggests that they represent fully liganded shut states. They are also relatively consistent between patches, which probably have varying numbers of active receptors which would be expected to cause variation in the shut times between receptor activations, but would not affect shut times within single activations. These gaps therefore provide useful information about the activation of the P2X receptor and suggest that during activation (e.g. during a synaptic current) the open probability of the receptor channel is high.

### Burst properties

Activation of P2X receptors occurred in bursts of openings, as well as single openings. This bursting behaviour has been observed in a wide range of ion channels, including nicotinic ACh receptors (Colquhoun & Sakmann, 1985; Mathie *et al.* 1991), NMDA receptors (Howe *et al.* 1991; Gibb & Colquhoun, 1992), GABA<sub>A</sub> receptors (MacDonald *et al.* 1989*b*) and glycine receptors (Twyman & MacDonald, 1991), and is consistent with the characteristics expected for a fast neurotransmitter receptor (Edmonds *et al.* 1995). There was no significant change in the mean burst length with increasing ATP concentration but there was a significant increase in the burst  $P_{\text{open}}$ .

The burst kinetics of ligand-gated ion channel receptors may determine the time course of decay of most synaptic currents in the brain (reviewed by Edmonds *et al.* 1995). To date, in the CNS, P2X receptor-mediated synaptic currents have been observed in the medial habenula (Edwards *et al.* 1992), the dorsal horn of the spinal cord (Bardoni *et al.*



1997) and the hippocampus (Pankratov *et al.* 1998). The mean burst length of both the large conductance (10 ms) and the flickery P2X receptor channel (11 ms) is shorter than the 18 ms decay time constant reported in the medial habenula (Edwards *et al.* 1997), and therefore it is possible, depending on the receptor first latency time (Edmonds *et al.* 1995), that burst kinetics like this could underlie the synaptic current observed in the habenula. In addition, the absence of rectification observed in hippocampal neurons is also observed for habenular synaptic currents (Edwards *et al.* 1997). However, the medial habenula synaptic currents are blocked by suramin and by  $\alpha,\beta$ -meATP (Edwards *et al.* 1992), indicating that receptors different from those observed in this study underlie purinergic transmission in the medial habenula. Experiments with outside-out patches from medial habenula neurons need to be performed to determine whether a purinoceptor similar to the large conductance hippocampal P2X receptor exists in the habenula, although the soma of medial habenula neurons may not express P2X receptors (S. Robertson & F. A. Edwards, personal communication). Likewise, experiments investigating purinergic synaptic transmission in the hippocampal granule cells need to be performed to investigate whether P2X receptors similar to those described here mediate a component of synaptic transmission in the dentate gyrus. Although P2X receptor-mediated synaptic currents have been observed in the CA1 field of the hippocampus (Pankratov *et al.* 1998), the single channel properties of CA1 P2X receptors have yet to be described. The decay time constants for these synaptic currents were not provided and nor was the sensitivity to suramin tested. CA1 cell P2X receptors were partially blocked by 10  $\mu$ M PPADS (60%) and by  $\alpha,\beta$ -meATP (20  $\mu$ M) and exhibited desensitisation (Pankratov *et al.* 1998). These two lines of evidence suggest that a P2X receptor distinct from that observed in this study mediates a component of synaptic transmission in the CA1 region of the hippocampus. The burst kinetics of the two types of P2X receptor in granule cells are not consistent with the decay time constant of purinergic EPSCs in the spinal cord (decay time constants of 4–44 ms; Bardoni *et al.* 1997) and therefore, given that the dorsal horn receptors are also blocked by suramin (100  $\mu$ M), it is likely that a different type of receptor underlies the decay of the purinergic synaptic current in the dorsal horn.

#### The subunit composition of hippocampal granule cell P2X receptors

The pharmacological and biophysical evidence presented in this study suggests that the large conductance P2X receptor in hippocampal granule cells is likely to be a heteromer made up of a combination of P2X<sub>4</sub> and P2X<sub>6</sub> subunits or possibly any three of P2X<sub>1</sub>, P2X<sub>2</sub>, P2X<sub>4</sub> and P2X<sub>6</sub>. Another, albeit less likely, possibility is that the large conductance P2X receptor is a homomer containing P2X<sub>4</sub> subunits. The large conductance P2X receptor was partially inhibited by suramin application (30% reduction of  $P_{\text{open}}$ ), consistent

with heteromeric P2X receptors consisting of the P2X<sub>4</sub> and P2X<sub>6</sub> receptor subunits (Lê *et al.* 1998a), but the degree of block was greater than that for recombinant P2X<sub>4</sub> homomers (Bo *et al.* 1995; but see Séguéla *et al.* 1996). Suramin is a competitive antagonist at some P2X receptors (Dunn & Blakeley, 1988; Blakeley *et al.* 1991), but the fact that suramin increases the single channel conductance shows that it is not competitive at granule cell P2X receptors.

In addition, the large conductance hippocampal P2X receptor was sensitive to  $\alpha,\beta$ -meATP, which is not consistent with the presence of homomeric P2X<sub>2</sub> or P2X<sub>5</sub> receptors, as these receptors are insensitive to  $\alpha,\beta$ -meATP (Brake *et al.* 1994; Collo *et al.* 1996). This line of evidence also makes it unlikely that the receptor is a homomer of P2X<sub>4</sub> subunits as  $\alpha,\beta$ -meATP is inactive when recombinant P2X<sub>4</sub> receptor subunits are expressed in oocytes (Bo *et al.* 1995), but is consistent with the receptor being a heteromer of P2X<sub>4</sub> and P2X<sub>6</sub> subunits as recombinant P2X<sub>4</sub> and P2X<sub>6</sub> receptor heteromers are activated by  $\alpha,\beta$ -meATP (Lê *et al.* 1998a). This, coupled with the fact that the 55 pS conductance observed for this channel is six times larger than the single channel conductance of homomeric P2X<sub>4</sub> receptor channels (9 pS; Evans, 1996) suggests that the large conductance hippocampal P2X receptor is indeed a heteromer. However, the results presented in this paper do not rule out the presence of other suramin-sensitive subunits contributing to the large conductance P2X receptor, provided binding of suramin to that subunit does not prevent receptor activation. For example, one possibility is that the receptor is a trimer of P2X<sub>2</sub>, P2X<sub>4</sub> and P2X<sub>6</sub> subunits.

The flickery channel has a similar single channel conductance (32 pS) to that observed in spinal sensory neurons (35 pS) by Krishtal *et al.* (1988). The difference in conductance could be attributable to the higher concentration of extracellular calcium ions used in this study (0.3 mM as opposed to 0.1 mM for Krishtal *et al.* 1988). If this is the case, then the flickery P2X receptor may be composed of similar subunits to those in sensory neurons. It has been demonstrated that dorsal root ganglion neurons express functional heteromeric P2X receptors composed of P2X<sub>2</sub> and P2X<sub>3</sub> receptor subunits (Lewis *et al.* 1995). However, the single channel characteristics of these receptors have not yet been determined, so it is not clear yet whether the flickery channel could be composed of these two subunits.

In conclusion, the results of this study demonstrate the presence of functional P2X ATP receptors in the dentate gyrus of the hippocampus. To date, this is the first detailed single channel analysis of P2X receptors in the CNS. The results demonstrate that activation of P2X receptors follows the same principles established for activation of other ligand-gated ion channels that mediate fast synaptic transmission, allowing P2X receptors to contribute to the diversity of synaptic mechanisms in the mammalian brain.

- ASCHER, P. & NOWAK, L. (1988). The role of divalent cations in the *N*-methyl-D-aspartate responses of mouse central neurones in culture. *Journal of Physiology* **399**, 247–266.
- BALCAR, V. J., LI, Y., KILLINGER, S. & BENNETT, M. R. (1995). Autoradiography of P2X ATP receptors in the rat brain. *British Journal of Pharmacology* **115**, 302–306.
- BARDONI, R., GOLDSTEIN, P. A., LEE, C. J., GU, J. & MACDERMOTT, A. B. (1997). P2X ATP receptors mediate fast synaptic transmission in the dorsal horn of the rat spinal cord. *Journal of Neuroscience* **17**, 5297–5304.
- BEAN, B. P. (1990). ATP-activated channels in rat and bullfrog sensory neurons: Concentration dependence and kinetics. *Journal of Neuroscience* **10**, 1–10.
- BEAN, B. P., WILLIAMS, C. A. & CEELEN, P. W. (1990). ATP activated channels in rat and bullfrog sensory neurons; current voltage relationship and single-channel behaviour. *Journal of Neuroscience* **10**, 11–19.
- BENHAM, C. D. & TSIEN, R. W. (1987). A novel receptor-operated  $\text{Ca}^{2+}$  channel activated by ATP in smooth muscle. *Nature* **328**, 275–278.
- BLAKELEY, A. G. H., BROCKBANK, J. E., KELLY, S. S. & PETERSEN, S. A. (1991). Effects of suramin on the concentration-response relationship of  $\alpha,\beta$ -methylene ATP in the mouse vas deferens. *Journal of Autonomic Pharmacology* **11**, 45–49.
- BO, X. & BURNSTOCK, G. (1994). Distribution of  $^3\text{H}$   $\alpha,\beta$ -methylene ATP binding sites in rat brain and spinal cord. *NeuroReport* **5**, 1601–1604.
- BO, X., ZHANG, Y., NASSAR, M., BURNSTOCK, G. & SCHOEPFER, R. (1995). A P2X purinoceptor cDNA conferring a novel pharmacological profile. *FEBS Letters* **375**, 129–133.
- BRAKE, A. J., WAGENBACH, M. J. & JULIUS, D. (1994). New structural motif for ligand-gated ion channels defined by an ionotropic ATP receptor. *Nature* **371**, 519–523.
- CHEN, C. C., AKOPIAN, A. N., SIVILOTTI, L., COLQUHOUN, D., BURNSTOCK, G. & WOOD, J. N. (1995). A P2X purinoceptor expressed by a subset of sensory neurons. *Nature* **377**, 428–431.
- CLOUES, R. (1995). Properties of ATP-gated channel recorded from rat sympathetic neurons: Voltage dependence and regulation by  $\text{Zn}^{2+}$  ions. *Journal of Neurophysiology* **73**, 312–319.
- COLLO, G., NORTH, R. A., KAWASHIMA, E., MERLO-PICH, R., NEIDHART, S., SURPRENANT, A. & BUELL, G. (1996). Cloning of P2X<sub>5</sub> and P2X<sub>6</sub> receptors, and the distribution and properties of an extended family of ATP-gated ion channels. *Journal of Neuroscience* **16**, 2495–2507.
- COLQUHOUN, D. & HAWKES, A. G. (1981). On the stochastic properties of single ion channels. *Proceedings of the Royal Society B* **211**, 205–235.
- COLQUHOUN, D. & HAWKES, A. G. (1982). On the stochastic properties of bursts of single ion channel openings and of clusters of bursts. *Philosophical Transactions of the Royal Society B* **300**, 1–59.
- COLQUHOUN, D. & SAKMANN, B. (1985). Fast events in single channel currents activated by acetylcholine and its analogues at the frog muscle end-plate. *Journal of Physiology* **369**, 501–557.
- COLQUHOUN, D. & SIGWORTH, F. J. (1995). Fitting and statistical analysis of single-channel records. In *Single-Channel Recording*, 2nd edn, ed. SAKMANN, B. & NEHER, E., pp. 483–587. Plenum Press, New York. Website: <http://www.ucl.ac.uk/Pharmacology/dc.html>
- DING, S. & SACHS, F. (1999). Single channel properties of P2X<sub>2</sub> purinoceptors. *Journal of General Physiology* **113**, 695–719.
- DUNN, P. M. & BLAKELEY, A. G. H. (1988). Suramin: a reversible P<sub>2</sub>-purinoceptor antagonist in the mouse vas deferens. *British Journal of Pharmacology* **93**, 243–245.
- EDMONDS, B., GIBB, A. J. & COLQUHOUN, D. (1995). Mechanisms of activation of glutamate receptors and the time course of excitatory synaptic currents. *Annual Review of Physiology* **57**, 495–519.
- EDWARDS, F. A., GIBB, A. J. & COLQUHOUN, D. (1992). ATP receptor-mediated synaptic currents in the central nervous system. *Nature* **359**, 114–147.
- EDWARDS, F. A., KONNERTH, A., SAKMANN, B. & TAKAHASHI, T. (1989). A thin slice preparation for patch clamp recordings from neurones of the mammalian central nervous system. *Pflügers Archiv* **414**, 600–612.
- EDWARDS, F. A., ROBERTSON, S. J. & GIBB, A. J. (1997). Properties of ATP-mediated synaptic transmission in the rat medial habenula. *Neuropharmacology* **36**, 1253–1268.
- EVANS, R. J. (1996). Single channel properties of ATP-gated cation channels (P2X receptors) heterologously expressed in Chinese hamster ovary cells. *Neuroscience Letters* **212**, 212–214.
- FABIATO, A. (1988). Computer programs for calculating total from specified free or free from specified total ionic concentration in aqueous solutions containing multiple metals and ligands. *Methods in Enzymology* **157**, 378–417.
- FIEBER, L. A. & ADAMS, D. J. (1991). Adenosine triphosphate-evoked currents in cultured neurones dissociated from rat parasympathetic cardiac ganglia. *Journal of Physiology* **434**, 239–256.
- FRIEL, D. D. (1988). An ATP-sensitive conductance in single smooth muscle cells from the rat vas deferens. *Journal of Physiology* **401**, 361–380.
- FRIEL, D. D. & BEAN, B. P. (1988). Two ATP-activated conductances in bullfrog atrial cells. *Journal of General Physiology* **91**, 1–27.
- GIBB, A. J. & COLQUHOUN, D. (1992). Activation of *N*-methyl-D-aspartate receptors by L-glutamate in cells dissociated from adult rat hippocampus. *Journal of Physiology* **456**, 143–179.
- HALLIDAY, F. C. & GIBB, A. J. (1997). Single-channel properties of P2X ATP receptors in rat cerebellar slices. *Journal of Physiology* **504.P**, 51P.
- HAMILL, O. P., MARTY, A., NEHER, E., SAKMANN, B. & SIGWORTH, F. J. (1981). Improved patch clamp techniques for high-resolution current recording from cells and cell free patches. *Pflügers Archiv* **391**, 85–100.
- HOWE, J. R., CULL-CANDY, S. G. & COLQUHOUN, D. (1991). Currents through single glutamate receptor channel in outside-out patches from rat cerebellar granule cells. *Journal of Physiology* **432**, 143–202.
- HOYLE, C. H. V. (1996). Purinergic cotransmission: parasympathetic and enteric nerves. *Seminars in the Neurosciences* **8**, 206–215.
- KHAKH, B. S., HUMPHREY, P. P. & HENDERSON, G. (1997). ATP-gated cation channels (P2X purinoceptors) in trigeminal mesencephalic nucleus neurons of the rat. *Journal of Physiology* **498**, 709–715.
- KIDD, E. J., GRAHAMES, C. B. A., SIMON, J., MICHEL, A. D., BARNARD, E. A. & HUMPHREY, P. P. A. (1995). Localization of P2X purinoceptor transcripts in the rat nervous system. *Molecular Pharmacology* **48**, 569–573.
- KIM, M., YOO, O. J. & CHOE, S. (1997). Molecular assembly of the extracellular domain of P2X<sub>2</sub>, an ATP-gated ion channel. *Biochemical and Biophysical Research Communications* **240**, 618–622.
- KRISHTAL, O. A., MARCHENKO, S. M. & OBUKHOV, A. G. (1988). Cationic channels activated by extracellular ATP in rat sensory neurons. *Neuroscience* **27**, 995–1000.
- LÊ, K.-T., BABINSKI, K. & SÉGUÉLA, P. (1998a). Central P2X<sub>4</sub> and P2X<sub>6</sub> channel subunits coassemble into a novel heteromeric ATP receptor. *Journal of Neuroscience* **18**, 7152–7159.

- LÊ, K.-T., VILLENEUVE, P., RAMJAUN, A. R., MCPHERSON, P. S., BEAUDET, A. & SÉGUÉLA, P. (1998*b*). Sensory presynaptic and widespread somatodendritic immunolocalization of central ionotropic P2X ATP receptors. *Neuroscience* **83**, 177–190.
- LEWIS, C., NEIDHART, S., HOLY, C., NORTH, R. A., BUELL, G. & SURPRENANT, A. (1995). Coexpression of P2X<sub>2</sub> and P2X<sub>3</sub> subunits can account for ATP-gated currents in sensory neurons. *Nature* **377**, 432–435.
- MACDONALD, J. F., MODY, I. & SALTER, M. W. (1989*a*). Regulation of N-methyl-D-aspartate receptors revealed by intracellular dialysis of murine neurones in culture. *Journal of Physiology* **414**, 17–34.
- MACDONALD, R. L., ROGERS, C. J. & TWYMAN, R. E. (1989*b*). Kinetic properties of the GABA<sub>A</sub> receptor main conductance state of mouse spinal cord neurones in culture. *Journal of Physiology* **410**, 479–499.
- MCMANUS, O. B., BLATZ, A. L. & MAGLEBY, K. L. (1987). Sampling, log binning, fitting, and plotting durations of open and shut intervals from single channels. *Pflügers Archiv* **410**, 530–553.
- MATEO, J., GARCIA-LECEA, M., MIRAS-PORTUGAL, M. & CASTRO, E. (1998). Ca<sup>2+</sup> signals mediated by P2X-type purinoceptors in cultured cerebellar Purkinje cells. *Journal of Neuroscience* **18**, 1704–1712.
- MATHIE, A., COLQUHOUN, D. & CULL-CANDY, S. G. (1991). Conductance and single channel currents through nicotinic acetylcholine receptor channels in rat sympathetic ganglion neurones. *Journal of Physiology* **439**, 717–750.
- NAKAZAWA, K. & HESS, P. (1993). Block by calcium of ATP-activated channels in Pheochromocytoma cells. *Journal of General Physiology* **101**, 377–392.
- NICKE, A., BAUMERT, H. G., RETTINGER, J., EICHELE, A., LAMBRECHT, G., MUTSCHLER, E. & SCHMALZING, G. (1998). P2X<sub>1</sub> and P2X<sub>3</sub> receptors form stable trimers: a novel structural motif of ligand-gated ion channels. *EMBO Journal* **11**, 3016–3028.
- PANKRATOV, Y., CASTRO, E., MIRAS-PORTUGAL, M. T. & KRISHTAL, P. (1998). A purinergic component of the excitatory postsynaptic current mediated by P2X receptors in the CA1 neurons of the rat hippocampus. *European Journal of Neuroscience* **10**, 3898–3902.
- SÉGUÉLA, P., HAGHIGHI, A., SOGHOMONIAN, J.-J. & COOPER, E. (1996). A novel neuronal P<sub>2X</sub> ATP receptor ion channel with widespread distribution in the brain. *Journal of Neuroscience* **16**, 448–455.
- SHEN, K.-Z. & NORTH, R. A. (1993). Excitation of rat locus coeruleus neurons by adenosine-5'-triphosphate: Ionic mechanism and receptor characterization. *Journal of Neuroscience* **13**, 894–901.
- SIGWORTH, F. J. & SINE, S. M. (1987). Data transformations for improved display and fitting of single-channel dwell time histograms. *Biophysical Journal* **52**, 1047–1054.
- SILINSKY, E. M. & GERZANICH, V. (1993). On the excitatory effects of ATP and its role as a neurotransmitter in coeliac neurons of the guinea pig. *Journal of Physiology* **464**, 197–212.
- SMITH, R. M. & MARTELL, A. E. (1982). *Critical Stability Constants*. Plenum Press, New York.
- SNEDDON, P., MCLAREN, G. J. & KENNEDY, C. (1996). Purinergic cotransmission: sympathetic nerves. *Seminars in the Neurosciences* **8**, 201–205.
- STOOP, R., THOMAS, S., RASSENDREN, F., KAWASHIMA, E., BUELL, G., SURPRENANT, A. & NORTH, R. A. (1999). Contribution of individual subunits to the multimeric P2X(2) receptor: estimates based on methanethiosulfonate block at T336C. *Molecular Pharmacology* **56**, 973–981.
- TORRES, G. E., EGAN, T. M. & VOIGT, M. M. (1999). Hetero-oligomeric assembly of P2X receptor subunits – specificities exist with regard to possible partners. *Journal of Biological Chemistry* **274**, 6653–6659.
- TWYMAN, R. E. & MACDONALD, R. L. (1991). Kinetic properties of the glycine receptor main and sub-conductance states of mouse spinal neurones in culture. *Journal of Physiology* **435**, 303–331.
- VALERA, S., HUSSY, N., EVANS, R. J., ADAMI, N., NORTH, R. A., SURPRENANT, A. & BUELL, G. (1994). A new class of ligand-gated ion channel defined by P2X receptor for extracellular ATP. *Nature* **371**, 516–519.
- VULCHANOVA, L., ARVIDSSON, U., RIEDL, M., WANG, J., BUELL, G., SURPRENANT, A., NORTH, R. A. & ELDE, R. (1996). Differential distribution of two ATP-gated ion channels (P<sub>2X</sub> receptors) determined by immunocytochemistry. *Proceedings of the National Academy of Sciences of the USA* **93**, 8063–8067.
- WONG, A. Y. C., BURNSTOCK, G. & GIBB, A. J. (1998). Characterization of P2X ATP receptor single-channel properties in outside-out patches from granule cells in slices of rat hippocampus. *Journal of Physiology* **511.P**, 17P.
- WONG, A. Y. C., BURNSTOCK, G. & GIBB, A. J. (1999). The effect of suramin on the single channel properties of P2X ATP receptors in outside-out patches from rat hippocampal granule cells. *Journal of Physiology* **518.P**, 120P.
- ZHOU, X. & GALLIGAN, J. J. (1996). P2X purinoceptors in cultured myenteric neurons of guinea-pig small intestine. *Journal of Physiology* **496**, 719–729.
- ZHOU, Z. & HUME, R. I. (1998). Two mechanisms for inward rectification of current flow through the purinoceptor P2X<sub>2</sub> class of ATP-gated channels. *Journal of Physiology* **507**, 353–364.

#### Acknowledgements

This work was supported by the MRC, the Royal Society and the Nuffield Foundation. A.Y.C.W holds a UCL Departmental PhD studentship.

#### Corresponding author

A. J. Gibb: Department of Pharmacology, University College London, Gower Street, London WC1E 6BT, UK.

Email: a.gibb@ucl.ac.uk

#### Author's present address

A. Y. C. Wong: Ion Channel Group, Department of Cell Physiology and Pharmacology, University of Leicester, PO Box 138, Leicester LE1 9HN, UK.